Energy & Buildings 296 (2023) 113416

Contents lists available at ScienceDirect

Energy & Buildings

journal homepage: www.elsevier.com/locate/enb

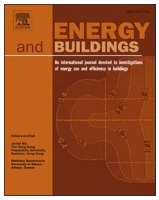

Quantification of the energy flexibility of residential building clusters: Impact of long-term refurbishment strategies of the italian building stock

A. Mugnini [a,*], F. Polonara [a,b], A. Arteconi [a,c]

[a] Dipartimento di Ingegneria Industriale e Scienze Matematiche, Università Politecnica delle Marche, Via Brecce Bianche 12, 60131, Ancona, Italy
[b] Consiglio Nazionale delle Ricerche, Istituto per le Tecnologie della Costruzione, Viale Lombardia 49, 20098, San Giuliano Milanese, MI, Italy
[c] Department of Mechanical Engineering, KU Leuven, B-3000, Leuven, Belgium

ARTICLE INFO

Keywords:
Energy flexibility
Buildings clusters
Flexibility quantification methods
Long-term refurbishment strategies
Italian building stock

ABSTRACT

A major refurbishment of the building stock is necessary to achieve the objectives of the energy transition. In addition to decreasing the overall energy demand, the energy efficiency of buildings can create a non-negligible reserve of flexibility and resilience for the entire energy system. Long-term refurbishment strategies can have an impact on such potential of the building sector that is still not widely exploited.

In this work the objective is to quantify the influence of long-term refurbishment strategies, planned until 2050, on the energy flexibility reserve of the entire building stock. Reference clusters of residential buildings have been modelled to represent the current and future scenarios of the Italian building stock. Lumped parameter models representing archetypes of residential buildings are implemented to represent the Italian building stock. Current statistics on the composition of the building stock have been combined with European refurbishment targets to 2050 to define the current and future scenarios of the Italian building stock.

Since the topic of quantifying the energy flexibility of clusters of buildings is still rather open, this study proposes an analysis based on a combination of different indicators derived from the literature and proposed ad hoc by the authors. They include flexibility curves, that correlate the demand of the cluster to the penalty signal (e.g., a price signal), and flexibility indicators for the comparison between the scenarios with and without activation of energy flexibility.

The results quantify the impact of Italian building stock refurbishment strategies on flexibility reserve and efficiency targets. It has been estimated that the maximum electrical power shiftable (both upward and downward) by activating the energy flexibility of the whole building stock can reach 17.9 GW_e in 2050. While in terms of energy, the following amounts of average daily shiftable energies have been obtained: from −34.4 to + 13.6 GWh_e in 2030, from −75.4 to + 16.2 GWh_e in 2040 and up to −113.5 to + 45.8 GWh_e in 2050, that represent around 2% of the present Italian electricity demand.

1. Introduction

The uncertainty on energy supply together with the need to reduce greenhouse gas emissions has made the energy transition increasingly urgent [1]. In this regard, the European Union has indicated the main objectives to increase the security and the sustainability of the energy system, namely the energy efficiency, the exploitation of Renewable Energy Sources (RESs) and the digitalization of the energy systems [2].

If from the point of view of energy efficiency, technological solutions are well known, the discussion regarding the consequences of a large dissemination of non-programmable RESs and the digitalization of the energy system is still open [3]. In fact, a large penetration of RESs, such as wind and photovoltaic, can strongly complicate the balance between energy demand and supply [4]. Due to the uncertainty of the energy supply, it will therefore be necessary to implement strategies to adapt demand to generation [5].

In this context buildings can play a key role since they account for about 40% of the total energy use [6]. In fact, buildings can exploit multiple energy carriers to meet the electrical and/or heat demand of the occupants. Examples are natural gas boilers for heating or electrically powered Heat Pumps (HPs) for air conditioning. Furthermore, buildings can have different levels of thermal inertia (e.g., from the thermal mass of the envelope [7,8], from highly inertial heating/cooling systems [9,10] or from dedicated thermal and/or electrical storage devices [11 12]) which allow to decouple the energy demand from the

* Corresponding author.
E-mail address: a.mugnini@univpm.it (A. Mugnini).

https://doi.org/10.1016/j.enbuild.2023.113416
Received 15 May 2023; Received in revised form 12 July 2023; Accepted 30 July 2023
Available online 1 August 2023

Nomenclature

Symbols

a	Index for the archetypes of buildings
ASSP	Average Stock Shiftable Power
BL	Baseline scenario
C	Thermal capacity (Wh K^{-1})
c	Cost of energy (EUR kWh^{-1})
CFI	Cluster Flexibility Indicator
COP	Coefficient of performance
CSE	Cluster Shiftable Energy
D	Number of avaliable archetypes of buildings
d	Number of days
DSM	Demand Side Management
ENEA	Italian National Agency for new technologies, energy and sustainable economic development
f	Input sharing factor
f(x)	Function that expresses the functional link between the change in demand and state of charge (33)
FX	Flexible scenario
G	Heat gains (W)
g(u)	Function that expresses the functional link between the change in demand and the price (33)
HP	Heat Pump
ISTAT	Italian National Statistical Institute
k	Time (hours)
MFH	Multi Family House
MSSP	Maximum Stock Shiftable Power
n	Number of each archetype in the cluster
N	Number of dwellings
PPD	Predicted Percentage of Dissatisfied
PUN	Single National Price
Q	Heating power (W)
R	Thermal Resistance (K W^{-1})
SFH	Single Family House
SFI	Stock Flexibility Indicator
SSE	Stock Shiftable Energy
T	Temperature (°C)
u	Normalized price
x	Normalized state of charge
Δk	Timestep (hours)

Subscripts

a	related to the single archetype
ai	related to indoor air node
air	related to indoor air
BL	related to the baseline scenario
cl	related to cluster
downward	related to downward (decreasing from baseline) power or energy shifts
e	related to electricity
f	related to floor
fins	related to the layer of the thermal insulation of the floor
fins	related to the layers of the floor which separate the thermal insulation from the indoor
fo	related to the layers of the floor which separate the external environment from the thermal insulation
FX	related to the flexible scenario
h	related to the heating system
HP	related to archetypes whit HP
i	related to internal gains
max	related to the maximum value
min	related to the minimum value
o	related to the outdoor environment
p	related to the layer of the internal partitions
pi	related to partitions
r	related to roof
ri	related to the layers of the roof which separate the thermal insulation from the indoor
rins	related to the layer of the thermal insulation of the roof
ro	related to the layers of the roof which separate the external environment from the thermal insulation
s	related to solar gains
sr	related to solar gains on roof
st	related to the whole building stock
sw	related to solar gains on external perimeter walls
w	related to external perimeter walls
wi	related to the layers of the perimeter walls which separate the thermal insulation from the indoor
winf	related to thermal resistance due to windows and natural ventilation
wins	related to the layer of the thermal insulation of the perimeter walls
wo	related to the layers of the perimeter walls which separate the external environment from the thermal insulation
upward	related to upward (increasing from baseline) power or energy shifts

supply [13].

The ability of a building to adapt its demand to variations in energy generation with limited effects on the comfort of the occupants is defined as Energy Flexibility. A definition of Energy Flexibility of buildings was introduced by Jensen et al. [14] as part of Annex 67: "*the energy flexibility of a building is the ability to manage its demand and generation according to local climate conditions, user needs, and energy network requirements*". According to this definition, the energy flexibility can be considered a characteristic of the building closely related to its intrinsic features (e.g., thermal losses or the level of thermal inertia available), but also to the boundary conditions. For instance, buildings with low thermal losses and a high level of thermal inertia can have a greater reserve of flexibility due to the long period in which the demand can be decoupled from generation [15].

Energy flexibility can also be linked to the topic of energy resilience [16]. Referring to a generic energy system, Roege et al. [17] provided a definition of energy resilience "*The ability of a system to recover from adversity*". Therefore, if the activation of the flexibility happens in normal operation, the resilience is a characteristic of the system in emergency contexts or during extreme events [16]. For buildings, flexibility and resilience can be considered closely related. Indeed, it is reasonable to assume that flexible buildings are also more resilient [18]. They can in fact guarantee the maintenance of the indoor comfort requirements for longer periods, therefore also in emergency situations [19].

Energy flexibility in buildings is a very hot topic in scientific literature. Several aspects were addressed, such as the identification of flexibility reserves [20 21], the assessment of different control techniques for the activation of the flexibility [22 23] or the identification of quantification methodologies [24 25]. Most of the available studies, however, focus on investigating the topic from the point of view of individual buildings. However, although it is essential to know the flexibility potential of a single building, in a recent paper Li et al. [18] highlighted how the most promising opportunities for energy flexibility are in clusters of buildings together with the possibility of exploiting multicarrier energy systems. In addition, at the size of clusters of buildings is also possible to appreciate the contribution in terms of resilience for the entire energy system [26].

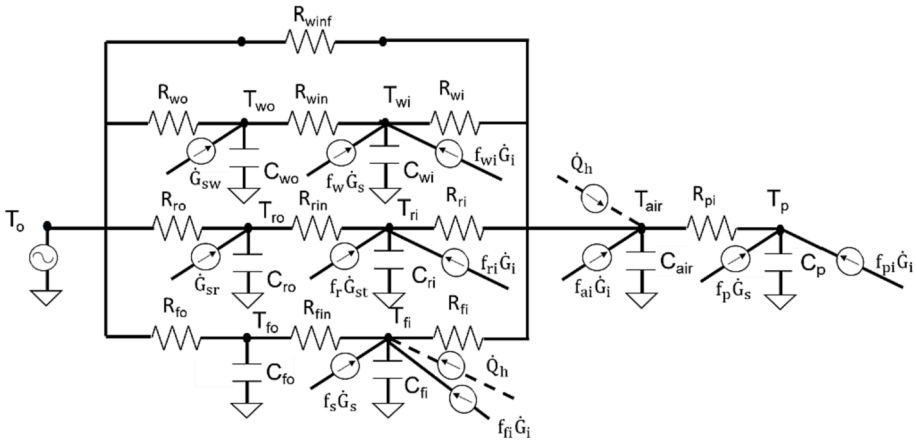

Fig. 1. RC-network to model the single archetype of residential dwelling.

Table 1
Dwellings in residential buildings by number of dwellings and construction period [41].

	Type of building: number of dwellings for each building					
Construction age	**1**	**2**	**3–4**	**5–8**	**9–15**	**16 and more**
before 1918	1′090′219	724′366	687′619	571′569	306′866	275′903
1919–1945	799′762	531′278	456′890	370′369	261′925	379′183
1946–1960	940′015	753′046	630′803	556′336	499′478	889′160
1961–1970	1′014′001	1′028′866	847′121	736′251	726′816	1′632′993
1971–1980	1′049′600	1′072′116	892′617	777′426	673′666	1′305′526
1981–1990	761′072	681′926	590′898	545′233	459′630	836′202
1991–2000	458′661	377′268	348′945	379′421	315′201	432′080
2001–2005	242′955	181′034	189′705	250′469	219′229	265′053
after 2006	185′461	126′690	150′054	222′238	198′402	238′665

Table 2
Percentage composition of the Italian building stock in terms of dwellings for the 2020 scenario. Dwellings divided by construction period and building type.

	SFH		**MFH**	
Construction age	Percentage of dwellings	Number of dwellings per building	Percentage of dwellings	Number of dwellings per building
Class 1 (before 1970)	12.1%	1	40.5%	4
Class 2 (from 1971 to 1990)	5.7%	1	24.7%	4
Class 3 (from 1991 to 2005)	2.2%	1	9.3%	5
Class 4 (from 2006 to 2015)	0.8%	1	3.8%	5
Class 5 (from 2016 onwards)	0.1%	1	0.7%	5

According to the definition proposed by Vigna et al [27], building clusters are groupings of buildings interconnected to the same energy infrastructure. This means that, as Vigna et al pointed out, every variation in the single building has an impact both on the energy infrastructure and on the other buildings in the cluster. In this sense, buildings can be physically connected (i.e., the exchange of energy takes place between the buildings or with a common energy source), or the connection can be at the level of the energy market (i.e., the management of the energy flows of the individual buildings are managed by an external market player) [28].

Some studies are emerging regarding the assessment of the energy flexibility of clusters of buildings. For instance, Kaspar et al [29] proposed a critical review of the control techniques to exploit Demand Side Management (DSM) in cluster of buildings. The authors highlighted how the most widespread strategy is a Multi-Agent System in which each building or each technology in the building behaves as an autonomous agent that acts according to a common objective. Another interesting study is proposed by Papachristou et al [30]. Here the authors estimated the flexible capacity of a cluster of Dutch office buildings. They concluded that the aggregated flexibility of the case study is comparable to large battery parks (10 MWh capacity managing with 17 office buildings). Tang et al [31], instead, proposed a decentralized control strategy based on game theory for managing the energy demand of a building cluster by exploiting the thermal mass of buildings. With the proposed strategy, the authors assessed an aggregated peak demand reduction potential of about 10% with an associated economic savings of 5%.

The works mentioned refer to specific case studies in which strategies for activating the energy flexibility deriving from the heating and cooling demand of clusters are evaluated. In contrast, there are not many works that address the topic of energy flexibility characterization in clusters. An interesting work in this direction is the one proposed by Vigna et al [28]. Here the authors analyzed several configurations of clusters composed of buildings with different thermal mass and thermal losses. Their results showed how flexible cluster management can enable up to 18% reduction in energy-related carbon emissions. Furthermore, Vigna et al [28] clearly showed how the flexibility potential of the cluster is strongly affected by the envelope configuration (i.e., by the thermal mass and thermal transmittance of the walls). Andrews and Jain [32] instead, propose a methodology to incorporate demand flexibility into the benchmarking of buildings. The authors applied their method to a case study consisting of 306 primary and secondary schools in Southern California, USA. With their results, they demonstrated how different building subsets can play a crucial role in decarbonization

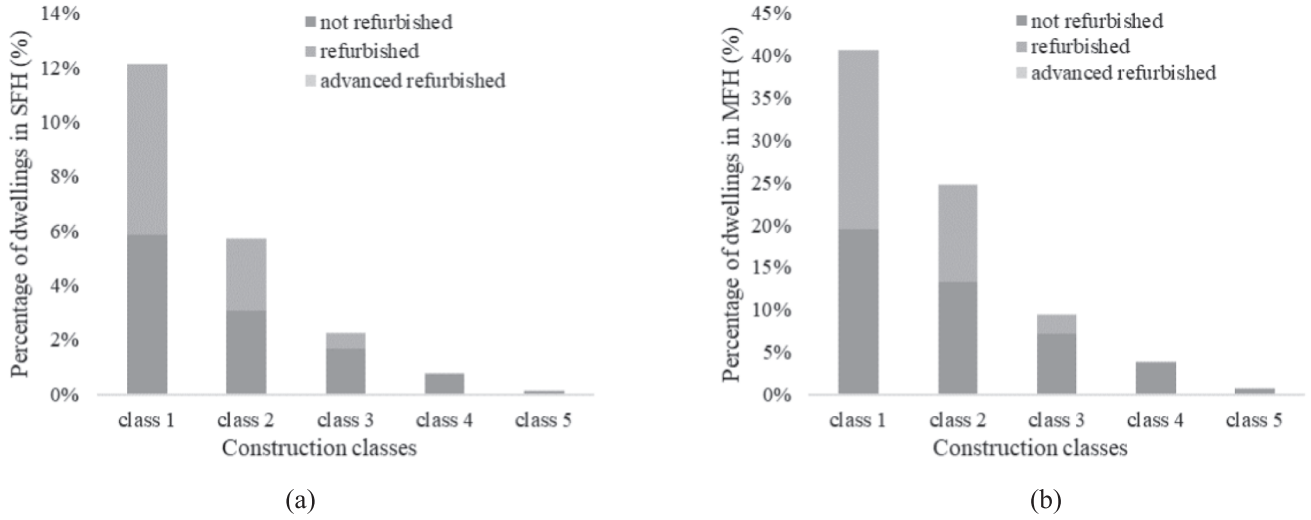

Fig. 2. Composition of the Italian buildings stock in the 2020 scenario in terms of dwellings: breakdown by construction period and state of refurbishment: (a) dwellings in SFH buildings and (b) dwellings in MFH buildings.

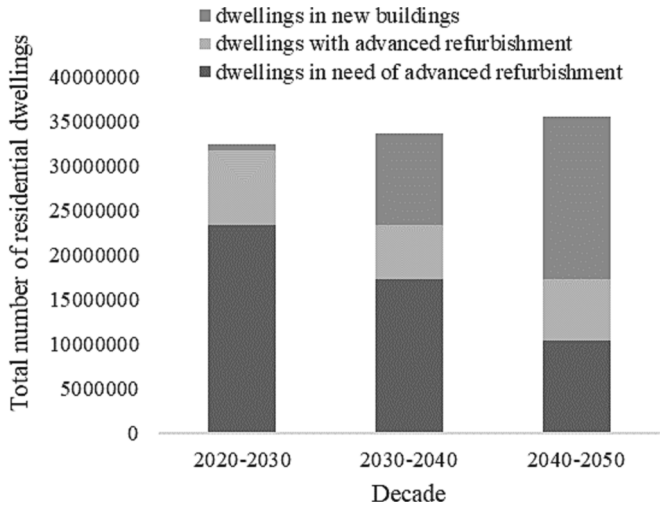

Fig. 3. Evolution of the composition of the building stock in the decades 2020–2030, 2030–2040 and 2040–2050. Breakdown between dwellings in new buildings, dwelling with and without advanced refurbishment.

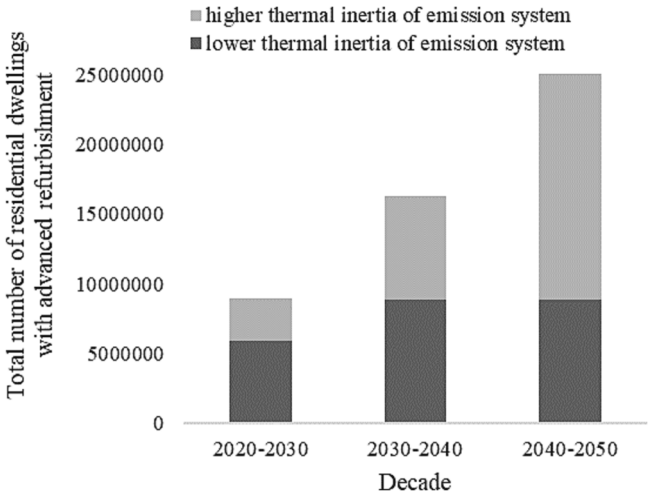

Fig. 4. Total number of residential dwellings with advanced refurbishment in the decades 2020–2030, 2030–2040 and 2040–2050. Breakdown between lower and higher thermal inertia emission system.

mainly due to their high flexibility in demand management. Besides presenting a method, Andrews and Jain highlighted the importance of energy flexibility, beyond efficiency, in the building stock of the future. Another interesting study demonstrating the importance of the availability of energy flexibility in clusters of buildings is that proposed by Amadeh et al [33]. The authors proposed a framework to characterize the operative flexibility of a cluster of 1000 residential buildings equipped with HPs. The introduced methodology makes it possible to obtain information about the real-time flexible capacity of the cluster and to generate information that can be used for bidding in the electricity market. The study proposes a characterization of cluster flexibility by modelling an equivalent virtual storage. However, this characterization has a purely operational purpose.

The analysis of the literature clearly shows the importance of energy demand flexibility in the composition of the future building stock. It is also clear from the literature that the actual available flexibility reserve in buildings should be characterized operationally. Against this background, this work aims to assess the impact of long-term renovation strategies on the reserve of flexibility that residential buildings can provide to the global energy system. The study proposes scenario analysis and aims to quantify the reserve of potential flexibility resulting from the implementation of the planned European strategies for the redevelopment of the building stock by 2050.

To quantify the energy flexibility, Vigna et al. [28] extended to the cluster level a methodology, based on the calculation of flexibility indicators, also proposed for single buildings. Considering this last assumption, this work intends to generalize the characterization of energy flexibility to clusters of residential buildings representative of the entire building stock. Focusing on the Italian case study, the effects of the involvement of the entire Italian building park in DSM programs in the current scenario and in future scenarios are quantified in this study. For the above considerations, the flexibility reserve can also provide an interesting order of magnitude on the resilience potential for the energy system.

In particular, in this work the current buildings scenario has been compared with future scenarios, resulting from the application of the planned long-term refurbishment strategies up to 2050. The scenarios were evaluated based on statistical data and on the recommendations of the European Union about the energy requalification of the buildings

Table 3
Thermal transmittance (in W m^{-2} K^{-1}) for external wall: distinction by construction class and state of building [37].

Construction age	Existing state		Usual refurbishment		Advanced refurbishment	
	SFH	MFH	SFH	MFH	SFH	MFH
Class 1 (before 1970)	1.70	1.48	0.33	0.33	0.25	0.25
Class 2 (from 1971 to 1990)	0.76	0.80	0.33	0.30	0.25	0.25
Class 3 (from 1991 to 2005)	0.59	0.59	0.31	0.31	0.25	0.24
Class 4 (from 2006 to 2015)	0.34	0.34	0.27	0.27	0.13	0.13
Class 5 (from 2016 onwards)	0.27	0.27	–	–	0.13	0.13

Table 4
Thermal transmittance (in W m^{-2} K^{-1}) for roof: distinction by construction class and state of building [37].

Construction age	Existing state		Usual refurbishment		Advanced refurbishment	
	SFH	MFH	SFH	MFH	SFH	MFH
Class 1 (before 1970)	2.20	1.65	0.30	0.30	0.22	0.21
Class 2 (from 1971 to 1990)	1.14	0.75	0.30	0.26	0.23	0.21
Class 3 (from 1991 to 2005)	0.57	0.57	0.27	0.27	0.21	0.21
Class 4 (from 2006 to 2015)	0.28	0.28	0.22	0.22	0.13	0.13
Class 5 (from 2016 onwards)	0.22	0.22	–	–	0.13	0.13

Table 5
Thermal transmittance (in W m^{-2} K^{-1}) for floor: distinction by construction class and state of building [37].

Construction age	Existing state		Usual refurbishment		Advanced refurbishment	
	SFH	MFH	SFH	MFH	SFH	MFH
Class 1 (before 1970)	2.00	1.30	0.30	0.30	0.24	0.21
Class 2 (from 1971 to 1990)	0.98	0.98	0.30	0.28	0.22	0.22
Class 3 (from 1991 to 2005)	0.63	0.77	0.28	0.30	0.22	0.22
Class 4 (from 2006 to 2015)	0.33	0.33	0.30	0.30	0.16	0.16
Class 5 (from 2016 onwards)	0.30	0.30	–	–	0.16	0.16

Table 6
Thermal transmittance (in W m^{-2} K^{-1}) for external windows: distinction by construction class and state of building [37].

Construction age	Existing state		Usual refurbishment		Advanced refurbishment	
	SFH	MFH	SFH	MFH	SFH	MFH
Class 1 (before 1970)	4.70	4.90	2.00		1.70	1.70
Class 2 (from 1971 to 1990)	2.80	3.70	2.00	2.00	1.70	1.70
Class 3 (from 1991 to 2005)	2.80	2.20	2.00	2.00	1.70	1.70
Class 4 (from 2006 to 2015)	2.20	2.20	1.80	1.80	1.10	1.10
Class 5 (from 2016 onwards)	1.80	1.80	–	–	1.10	1.10

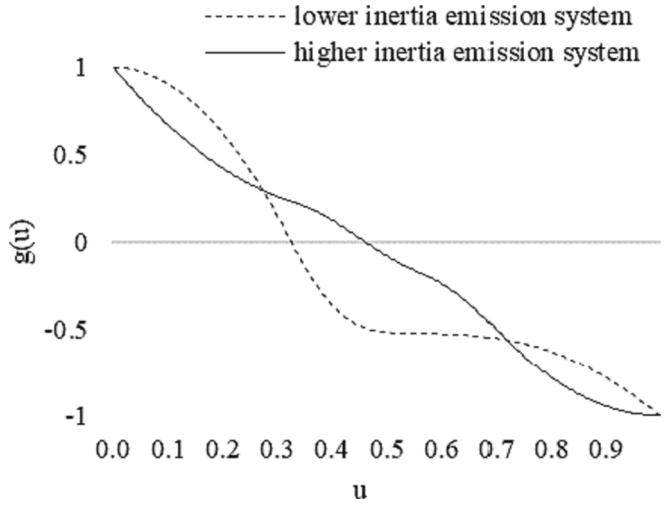

Fig. 5. Comparison between flexibility characterization [35] of SFH (class 3 with advanced refurbishment) with lower thermal inertia emission system (i.e., radiators) and higher thermal inertia emission system (i.e., underfloor): functional relationships between the energy price and the energy demand.

[34]. The quantification of energy flexibility was achieved both through the methodology proposed by Junker et al. [35], already applied for single buildings, and through flexibility indicators proposed by the authors.

To conclude, the innovative aspects of this study, compared to what is available in the literature, can be summarized as follows. First, to contribute to increasing knowledge on the topic of the quantification of energy flexibility in clusters. Then, to demonstrate the urgency of a large-scale implementation of the policies of renovation of the building stock. This second aspect is highlighted by the estimated benefits that can be obtained for the energy system from the exploitation of such a reserve of flexibility. Accordingly, this study aims to help address the following open research challenges:

- How to quantify the reserve of energy flexibility obtainable from the activation of the thermal mass in cluster of buildings?
- What is the impact of long-term building stock refurbishment policies on the flexibility reserve that can be provided to the grid?
- Demonstrate how different types of buildings and heating/cooling systems contribute differently to the potential flexibility reserve of the building stock.

Table 7
Electricity consumption and cost: comparison between baseline and flexible scenario: lower and higher thermal inertia emission systems (SFH, class C3 with advanced refurbishment). Month of January.

	Baseline scenario		Flexibility scenario	
	Lower thermal inertia emission system	Higher thermal inertia emission system	Lower thermal inertia emission system	Higher thermal inertia emission system
Electricity (kWh)	1208	819	1215	832
Electricity cost (EUR)	272	185	269	172

In this sense, the analysis proposed in this work aims also to provide estimates of flexibility potential to encourage an acceleration towards the energy requalification of the buildings sector. In fact, as the European Commission's statistical observer estimates, at least 75 % of European buildings was energy inefficient in 2020 [36].

The paper is structured as follows: in Section 2 the methodology is described. The methodology contains the description of the model of the single buildings, the definition of the reference and the flexible scenario and finally the energy flexibility quantification methods. Section 3 contains the description of the scenarios for the Italian building stock in the current and future evolutions. In Section 4 the clusters identified as representative case studies are presented, while in Section 5 the results are described. Finally, the main conclusions are summarized in Section 6.

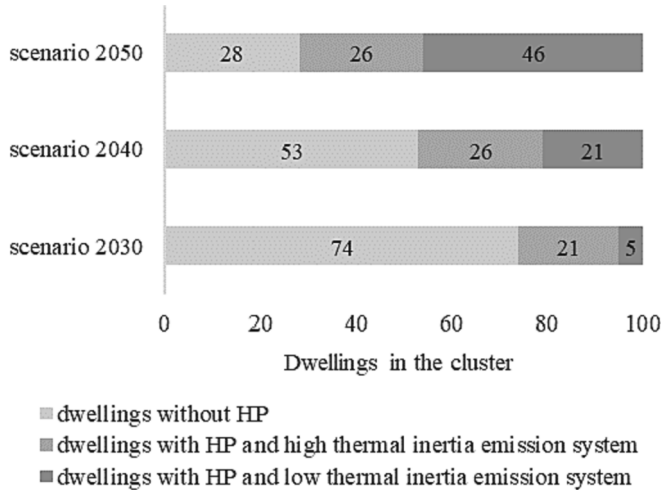

Fig. 6. Composition of the cluster in future scenarios: distinction between buildings without HP and with HP between the different emission systems (low and high thermal inertia).

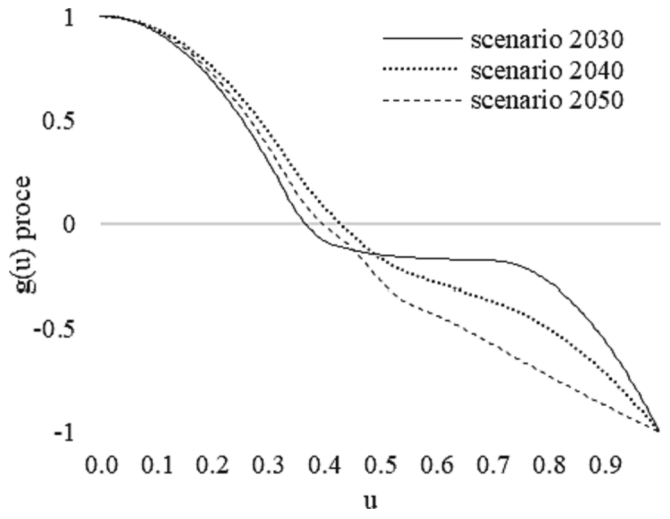

Fig. 7. Comparison between flexibility characterization [35] of the cluster in future scenarios: functional relationships between the energy price and the energy demand.

2. Methodology

In this section, the methodologies used to obtain the energy demand of the clusters and to quantify their flexibility reserve are presented. Subsections 2.1 contains details of the single building modeling while subsection 2.2 explains how the flexible and the reference scenarios are obtained. Then, subsection 2.3 describes the flexibility quantification methodologies.

2.1. Single buildings model

The individual buildings composing the cluster represent archetypes of reference dwellings for the Italian building stock. The archetypes are modeled with networks of resistances and capacitances (i.e., RC networks) whose parameters are obtained through a white box approach starting from the data reported in the Tabula Project [37]. Fig. 1 shows a general scheme of the RC-network.

According to Boodi et al [38] each external wall is modeled with a network of 3 resistances and 2 capacitances (i.e., 2 thermal nodes). The two nodes refer to the temperature of the walls before the thermal insulation (i.e., facing the internal air zone, T_{air}) and after the thermal insulation (i.e., facing the outdoor environment, T_o). These are respectively: T_{wi} and T_{wo} for the vertical walls, T_{ri} and T_{ro} for the roof and T_{fi} and T_{fo} for the floor. The thermal capacitances referred to the thermal nodes described above, therefore, refer to the sum of the layers of the stratigraphy of the walls towards the inside (i.e., the layers from the thermal insulation to the thermal node of the indoor air T_{air}) and towards the outside (i.e., layers from the thermal insulation to T_o). These are: C_{wi} and C_{wo} for the vertical walls, C_{ri} and C_{ro} for the roof and C_{fi} and C_{fo} for the floor. As far as the thermal resistances are concerned, these represent the equivalent thermal resistances due to the layers of the envelope which are located between T_{air} and the thermal insulation (R_{wi} for the vertical walls, R_{ri}, for the roof and R_{fi} for the floor), the resistance of the thermal insulation (R_{win} for the vertical walls, R_{rin}, for the roof and R_{fin} for the floor) and the equivalent resistance from the layer of the thermal insulation to T_o (R_{wo} for the vertical walls, R_{ro}, for the roof and R_{fo} for the floor). In some cases, there is also an additional node which represents internal walls (C_p, T_p), in this case R_p represents the thermal resistance of the stratigraphy of the internal partition. R_{winf} represents, instead, the thermal resistance of the windows and due to natural ventilation (assumed equal to 0.5 hr^{-1} for all the archetypes). Sensible internal gains ($\dot{G}_i$) are 60% radiative and 40% convective (only internal gains due only to occupation and considered constant throughout the day are modeled). This last is assigned to the indoor air node (f_{ai} equal to 0.4 in Fig. 1) [39]. The radiative contribution is instead uniformly distributed, according to the area occupied by the surfaces, among the internal surfaces (f_{pi}, f_{wi}, f_{ri} and f_{fi} in Fig. 1). Two types of solar gains are considered: (i) the solar gains due to solar radiation absorbed by the

Table 8
Electricity consumption and cost: comparison between baseline and flexible scenario.

	Baseline scenario			Flexibility scenario		
	Scenario 2030	Scenario 2040	Scenario 2050	Scenario 2030	Scenario 2040	Scenario 2050
Electricity (kWh)	14,564	27,872	36,777	12,572	22,405	30,858
Electricity cost (EUR)	3290	6275	8287	2705	4833	6565

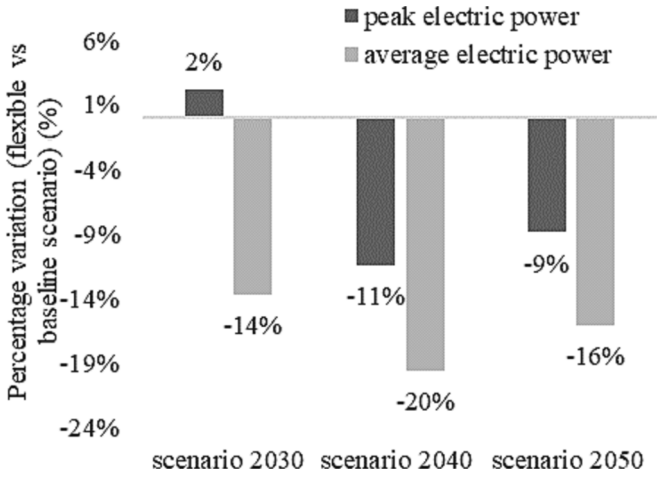

Fig. 8. Comparison between flexible scenario and baseline in the future scenarios: percentage variation of the electricity peak power and average electricity power (month of January).

external surfaces of the building envelope ($\dot{G}_{sw}$, $\dot{G}_{sr}$ and $\dot{G}_{sf}$) and due to the solar radiation transmitted by the windows ($\dot{G}_s$). The latter are distributed between the internal surface of the envelope according to constant interior solar distribution fractions (f_w, f_r, f_f and f_p in Fig. 1) [39]. Finally, the thermal power supplied by the heating system ($\dot{Q}_h$) is attributed either to the thermal node of the air (to model a low thermal inertia emission system such as radiators) or to the internal thermal node of the floor (to model an emission system with higher thermal inertia such as underfloor heating). More details on this in relation to specific case studies will be provided in Section 4. The model for the single building was validated using the BESTEST method [39].

2.2. Baseline and flexible scenario

Different optimization problems are solved to obtain the thermal dynamics and energy needs of buildings in the clusters. For each cluster two operating conditions are defined: the baseline (i.e., without activation of flexibility) and the flexible scenario. The baseline is obtained as the sum of the results of single optimization problems evaluated for single archetypes. Equation (1) reports the objective function that is minimized for each archetype (a) where k is the time (a timestep of 1 h is used).

$$\min \sum_{k}^{k_{tot}} \dot{Q}_a(k)\Delta k \tag{1}$$

subjected to:

$$0 \le \dot{Q}_a(k) \le \dot{Q}_{a,max} \tag{2}$$

$$T_{air,min\,BL} \le T_{a,air}(k) \le T_{air,max\,BL} \tag{3}$$

where Equation (2) represents the boundary conditions for the decision variables (i.e., the thermal power of heating for each archetype, $\dot{Q}_a$) and Equation (3) the constraints on the internal air temperature of each archetype a ($T_{a,air}$). The latter constraint imposes that the air temperature must be maintained within the limits of the thermostat ($T_{air,min\,BL}$ and $T_{air,max\,BL}$), while Equation (2) requires that $\dot{Q}_a$ does not exceed the maximum power, evaluated as the nominal thermal load of each archetype.

The thermal power of the cluster in the baseline scenario ($\dot{Q}_{BL}$) is given by the sum of the thermal powers of the individual archetypes (according to the number of each archetype in the cluster, n_a):

$$\dot{Q}_{BL}(k) = \sum_{a}^{D_a} n_a \dot{Q}_a(k) \tag{4}$$

where D_a is the number of available archetypes.

On the other hand, the flexible scenario involves solving a single optimization problem for the cluster. As the flexibility analyses proposed in this study focuses on the activation of energy flexibility resulting from heat demand for space heating, the flexible scenario involves only the archetypes that foresee HPs as generation system. A price signal (c_e) is chosen as forcing function. Thus, the objective function in the flexible scenario is the minimization of the cost of electricity demand of the cluster:

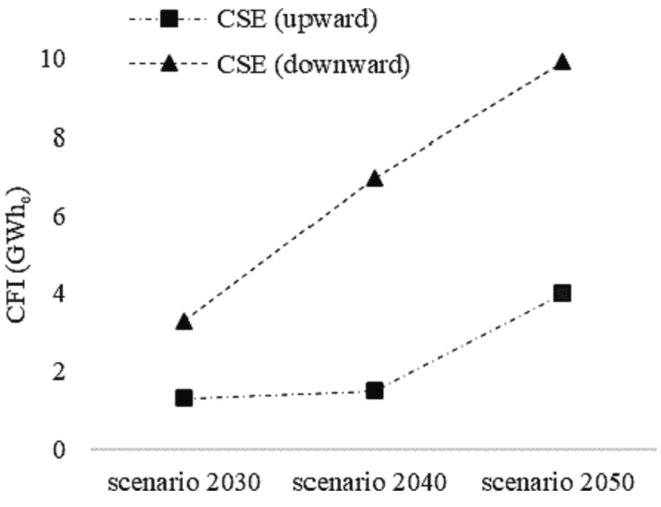

Fig. 9. Comparison between future scenarios in terms of CFIs.

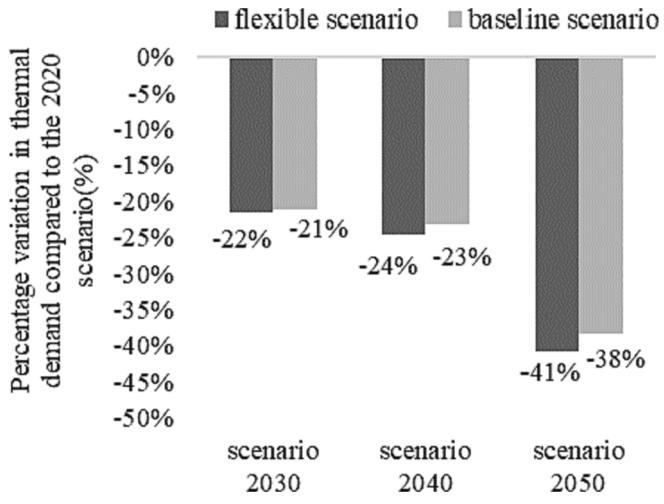

Fig. 10. Percentage variations in cluster thermal demand compared to 2020 scenario: assessment for both baseline and flexible scenarios.

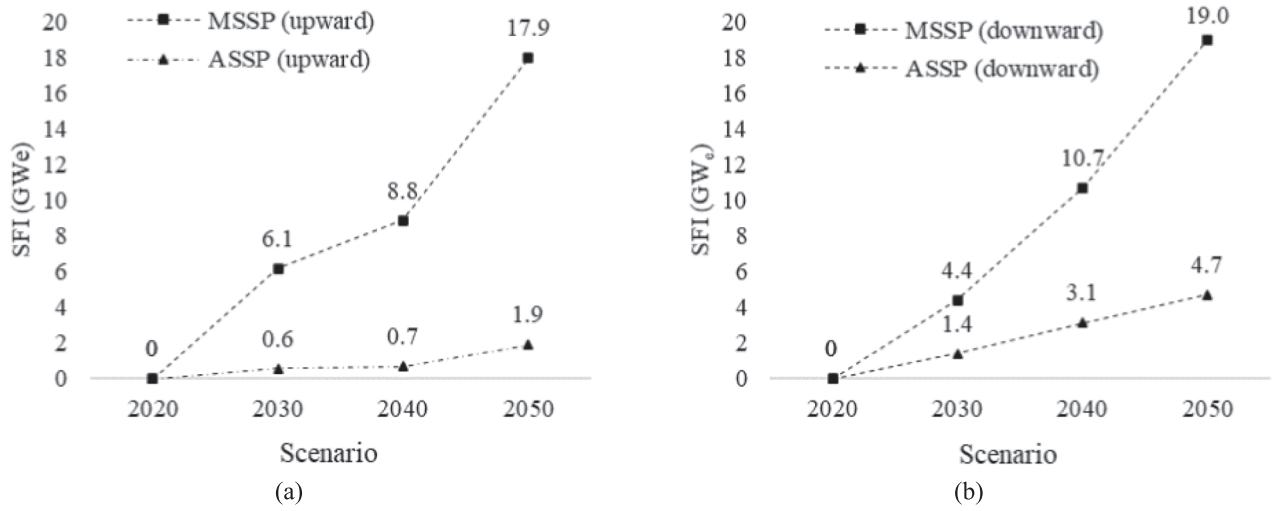

Fig. 11. SFIs in terms of shiftable power: (a) power shifts increasing compared to the baseline and (b) power shifts decreasing compared to the baseline.

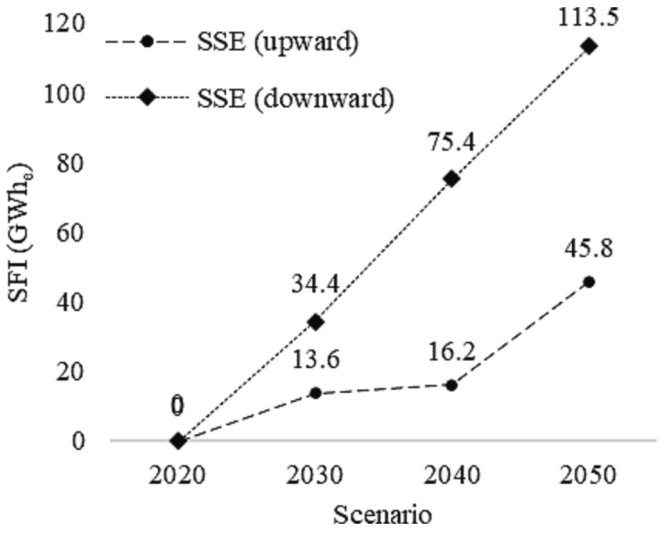

Fig. 12. SFIs in terms of shiftable energy.

Table 9
Impact of the minimum, average and maximum power used by the HP in the different scenarios in relation to the minimum global Italian electricity demand (data referring to January 2022).

	Impact of electricity demand for HP (%)		
	Minimum	Average	Maximum
Scenario 2030	1 %	3 %	6 %
Scenario 2040	2 %	7 %	13 %
Scenario 2050	2 %	9 %	18 %

$$\min \sum_{a}^{D_{aHP}} \left[\sum_{k}^{k_{tot}} n_a c_e(k) \frac{\dot{Q}_a(k)}{COP_a(k)} \Delta k \right] \quad (5)$$

where COP_a is the Coefficient of Performance (COP) of the HP in each archetype (a) and D_{aHP} is the number of archetypes available with HP. The COP varies according to the outdoor air temperature and the supply temperature. The performance curves were extrapolated from manufacturer data for a real air source HP [40]. The supply temperature has been assumed fixed and dependent on the type of emission system: 55 °C for the low inertia emission system and 35 °C for the case with the highest thermal inertia. Also, in this case Equation (2) is applied to each dwelling in the cluster, while the constraints on the indoor air temperature are modified as follows:

$$T_{air,min\,FX} \leq T_{a,air}(k) \leq T_{air,max\,FX} \quad (6)$$

To avoid that the optimization problem always evaluates indoor air temperatures too low, the following condition was set to $T_{air,min\,FLEX}$:

$$\begin{cases} \text{if } c_e(k) \rangle \left\{ \max(c_e) - \left[\frac{\max(c_e) - \min(c_e)}{4} \right] \right\} & T_{air,min\,FX}(k) = T_{air,min\,BL} - 1\,^{\circ}C \\ \text{if } c_e(k) \leq \left\{ \max(c_e) - \left[\frac{\max(c_e) - \min(c_e)}{4} \right] \right\} & T_{air,min\,FX}(k) = T_{air,min\,BL} \end{cases} \quad (7)$$

Through Equation (7) buildings are allowed to be able to lower the

Table A1
Numerical values of the parameters for archetypes in class 1 (SFH).

	existing state	usual refurbishment	advanced refurbishment
R_{winf} (K W^{-1})	0.0062	0.0097	0.0103
R_{wo} (K W^{-1})	0.0002	0.0004	0.0004
R_{win} (K W^{-1})	–	0.0136	0.0187
R_{wi} (K W^{-1})	0.0036	0.0035	0.0035
C_{wo} (Wh K^{-1})	31,657	1820	1849
C_{wi} (Wh K^{-1})	–	29,916	29,916
R_{ro} (K W^{-1})	0.0005	0.0008	0.0008
R_{rin} (K W^{-1})	–	0.0355	0.0494
R_{ri} (K W^{-1})	0.0051	0.0051	0.0051
C_{ro} (Wh K^{-1})	6728	920	964
C_{ri} (Wh K^{-1})	–	6728	6728
R_{fo} (K W^{-1})	0.0003	0.0019	0.0015
R_{fin} (K W^{-1})		0.0364	0.0463
R_{fi} (K W^{-1})	0.0058	0.003	0.0034
C_{fo} (Wh K^{-1})	23,648	14,355	4410
C_{fi} (Wh K^{-1})	–	4174	4411
C_{air} (Wh K^{-1})	250	250	250
f_w (-)	0.2248	0.2248	0.2266
f_{wi} (-)	0.3108	0.3108	0.3108
f_r (-)	0.1238	0.1238	0.1245
f_{ri} (-)	0.1446	0.1446	0.1446
f_f (-)	0.6387	0.6387	0.6395
f_{fi} (-)	0.1446	0.1446	0.1446
f_{ai} (-)	0.4	0.4	0.4

Table A2
Numerical values of the parameters for archetypes in class 2 (SFH).

	existing state	usual refurbishment	advanced refurbishment
R_{winf} (K W^{-1})	0.0068	0.0079	0.0084
R_{wo} (K W^{-1})	0.0036	0.0036	0.0036
R_{win} (K W^{-1})	0.0015	0.0105	0.0152
R_{wi} (K W^{-1})	0.0018	0.0018	0.0018
C_{wo} (Wh K^{-1})	15,150	15,220	15,257
C_{wi} (Wh K^{-1})	4499	4499	4499
R_{ro} (K W^{-1})	0.0006	0.0006	0.0006
R_{rin} (K W^{-1})	0.004	0.0289	0.0389
R_{ri} (K W^{-1})	0.0042	0.0042	0.0042
C_{ro} (Wh K^{-1})	1014	1131	1178
C_{ri} (Wh K^{-1})	8264	8264	8264
R_{fo} (K W^{-1})	0.0032	0.0032	0.0012
R_{fin} (K W^{-1})	0.0044	0.0276	0.0427
R_{fi} (K W^{-1})	0.0025	0.0025	0.0028
C_{fo} (Wh K^{-1})	5094	5138	5417
C_{fi} (Wh K^{-1})	4630	4630	5428
C_{air} (Wh K^{-1})	308	308	308
f_w (-)	0.2152	0.2152	0.2169
f_{wi} (-)	0.2935	0.2935	0.2935
f_r (-)	0.1327	0.1327	0.1335
f_{ri} (-)	0.1532	0.1532	0.1532
f_f (-)	0.6394	0.6394	0.6402
f_{fi} (-)	0.1532	0.1532	0.1532
f_{ai} (-)	0.4	0.4	0.4

Table A3
Numerical values of the parameters for archetypes in class 3 (SFH).

	existing state	usual refurbishment	advanced refurbishment
R_{winf} (K W^{-1})	0.0079	0.0091	0.0097
R_{wo} (K W^{-1})	0.0003	0.0003	0.0003
R_{win} (K W^{-1})	0.0072	0.0155	0.0199
R_{wi} (K W^{-1})	0.002	0.002	0.002
C_{wo} (Wh K^{-1})	1838	1895	1925
C_{wi} (Wh K^{-1})	16,946	16,946	16,946
R_{ro} (K W^{-1})	0.0007	0.0007	0.0007
R_{rin} (K W^{-1})	0.0148	0.0378	0.0494
R_{ri} (K W^{-1})	0.0048	0.0048	0.0048
C_{ro} (Wh K^{-1})	912	993	1033
C_{ri} (Wh K^{-1})	7143	7143	7143
R_{fo} (K W^{-1})	0.0037	0.0037	0.0014
R_{fin} (K W^{-1})	0.0119	0.0349	0.0494
R_{fi} (K W^{-1})	0.0029	0.0029	0.0032
C_{fo} (Wh K^{-1})	4412	4445	4682
C_{fi} (Wh K^{-1})	4001	4001	4692
C_{air} (Wh K^{-1})	266	266	266
f_w (-)	0.2242	0.2242	0.226
f_{wi} (-)	0.3059	0.3059	0.3059
f_r (-)	0.1254	0.1254	0.1261
f_{ri} (-)	0.1471	0.1471	0.1471
f_f (-)	0.638	0.638	0.6387
f_{fi} (-)	0.1471	0.1471	0.1471
f_{ai} (-)	0.4	0.4	0.4

setpoint only at times when the cost is high. In fact, by widening the lower limit of the thermostat for each k the optimizer would still prefer to keep the indoor temperature as low as possible regardless of the price (Equation (5)).

For the archetypes without HP, the thermal dynamic and the heating demand are obtained as for the baseline scenario (Equations (1)-(3)). The overall thermal power of the cluster in the flexibility scenario ($\dot{Q}_{FX}$) is obtained with the same formulation expressed by Equation (4).

Given the linearity of the optimization problems, they are solved as Linear Programming optimization problems.

Table A4
Numerical values of the parameters for archetypes in class 4 (SFH).

	existing state	usual refurbishment	advanced refurbishment
R_{winf} (K W^{-1})	0.0087	0.0094	0.011
R_{wo} (K W^{-1})	0.0038	0.0038	0.0038
R_{win} (K W^{-1})	0.0105	0.0148	0.0371
R_{wi} (K W^{-1})	0.002	0.002	0.002
C_{wo} (Wh K^{-1})	14,365	14,395	14,548
C_{wi} (Wh K^{-1})	4597	4597	4597
R_{ro} (K W^{-1})	0.0007	0.0007	0.0007
R_{rin} (K W^{-1})	0.0358	0.046	0.0817
R_{ri} (K W^{-1})	0.0053	0.0053	0.0053
C_{ro} (Wh K^{-1})	1014	1056	1200
C_{ri} (Wh K^{-1})	10,923	10,923	10,923
R_{fo} (K W^{-1})	0.004	0.004	0.0014
R_{fin} (K W^{-1})	0.0281	0.0319	0.0661
R_{fi} (K W^{-1})	0.0029	0.0029	0.0022
C_{fo} (Wh K^{-1})	10,147	10,153	4737
C_{fi} (Wh K^{-1})	4048	4048	5545
C_{air} (Wh K^{-1})	269	269	269
f_w (-)	0	0	0.2259
f_{wi} (-)	0	0	0.305
f_r (-)	0.2242	0.2242	0.1264
f_{ri} (-)	0.305	0.305	0.1475
f_f (-)	0.1257	0.1257	0.6385
f_{fi} (-)	0.1475	0.1475	0.1475
f_{ai} (-)	0.4	0.4	0.4

Table A5
Numerical values of the parameters for archetypes in class 5 (SFH).

	existing state	advanced refurbishment
R_{winf} (K W^{-1})	0.0094	0.011
R_{wo} (K W^{-1})	0.0038	0.0038
R_{win} (K W^{-1})	0.0148	0.0371
R_{wi} (K W^{-1})	0.002	0.002
C_{wo} (Wh K^{-1})	14,395	14,548
C_{wi} (Wh K^{-1})	4597	4597
R_{ro} (K W^{-1})	0.0007	0.0007
R_{rin} (K W^{-1})	0.046	0.0817
R_{ri} (K W^{-1})	0.0053	0.0053
C_{ro} (Wh K^{-1})	1056	1200
C_{ri} (Wh K^{-1})	10,923	10,923
R_{fo} (K W^{-1})	0.004	0.0014
R_{fin} (K W^{-1})	0.0319	0.0661
R_{fi} (K W^{-1})	0.0029	0.0022
C_{fo} (Wh K^{-1})	10,153	4737
C_{fi} (Wh K^{-1})	4048	5545
C_{air} (Wh K^{-1})	269	269
f_w (-)	0.2242	0.2259
f_{wi} (-)	0.305	0.305
f_r (-)	0.1257	0.1264
f_{ri} (-)	0.1475	0.1475
f_f (-)	0.6378	0.6385
f_{fi} (-)	0.1475	0.1475
f_{ai} (-)	0.4	0.4

2.3. Energy flexibility quantification

Two methods have been used to quantify the energy flexibility of the clusters. The first is based on the characterization proposed by Junker et al [35]. In particular, Junker et al. proposed a quantification methodology applicable to any energy system whose flexibility is activated by a penalty function. Their method makes it possible to assess the capability

Table A6
Numerical values of the parameters for archetypes in class 1 (MFH in existing state).

	Dwelling 1	Dwelling 2	Dwelling 3	Dwelling 4
Orientation	Ground floor (windows on perimeter walls facing north, south and west)	Ground floor (windows on perimeter walls facing north, south and east)	First floor (windows on perimeter walls facing north, south and west)	First floor (windows on perimeter walls facing north, south and east)
R_{winf} (K W^{-1})	0.0108	0.0108	0.0108	0.0108
R_w (K W^{-1})	0.0008	0.0008	0.0008	0.0008
C_w (Wh K^{-1})	8612.0	8612.0	8612.0	8612.0
R_r (K W^{-1})	–	–	0.0005	0.0005
C_r (Wh K^{-1})	–	–	17,667	17,667
R_{fo} (K W^{-1})	0.0005	0.0005	–	–
C_f (Wh K^{-1})	18,078	18,078	–	–
C_{air} (Wh K^{-1})	124	124	124	124
R_{pi} (K W^{-1})	0.0043	0.0043	0.0043	0.0043
C_p (Wh K^{-1})	11,774	11,774	11,774	11,774
f_w (-)	0.1538	0.1538	0.1538	0.1538
f_{wi} (-)	0.1107	0.1107	0.1107	0.1107
f_r (-)	0	0	0.1558	0.1558
f_{ri} (-)	0	0	0.1481	0.1481
f_f (-)	0.6712	0.6712	0	0
f_{fi} (-)	0.1481	0.1481	0	0
f_{ai} (-)	0.4	0.4	0.4	0.4
f_{pi} (-)	0.1558	0.1558	0.6712	0.6712
f_p (-)	0.3412	0.3412	0.3412	0.3412

of the system to vary its energy demand according to the penalty (typically a price signal) and the state of charge of the system. The results of the application of the methodology are two functions: g(u) and f(x), obtained through a data-driven approach that assumes knowledge of historical building data with and without flexibility activation. The two functions g(u) and f(x) allow to extrapolate the link between the building response (i.e., evaluated in terms of flexibility activation) and the price signal (u) and building charge state (x), respectively. Moreover, this methodology estimates the share of the flexible demand.

In addition, some flexibility indicators defined by the authors have been calculated. Two types of indicators are defined: the Cluster Flexibility Indicators (CFIs) and the Stock Flexibility Indicators (SFIs). The CFIs refer to the evaluation of the results obtained for the modeled clusters (i.e., representative clusters). The SFIs, instead, are based on the

Table A7
Numerical values of the parameters for archetypes in class 1 (MFH in usual refurbishment).

	Dwelling 1	Dwelling 2	Dwelling 3	Dwelling 4
Orientation	*Ground floor (windows on perimeter walls facing north, south and west)*	*Ground floor (windows on perimeter walls facing north, south and east)*	*First floor (windows on perimeter walls facing north, south and west)*	*First floor (windows on perimeter walls facing north, south and east)*
R_{winf} (K W^{-1})	0.0179	0.0179	0.0179	0.0179
R_{wo} (K W^{-1})	0.0013	0.0013	0.0013	0.0013
R_{win} (K W^{-1})	0.0501	0.0501	0.0501	0.0501
R_{wi} (K W^{-1})	0.0129	0.0129	0.0129	0.0129
C_{wo} (Wh K^{-1})	495	495	495	495
C_{wi} (Wh K^{-1})	8138	8138	8138	8138
R_{ro} (K W^{-1})	0.0008	0.0008	0.0008	0.0008
R_{rin} (K W^{-1})	0.0343	0.0343	0.0343	0.0343
R_{ri} (K W^{-1})	0.0068	0.0068	0.0068	0.0068
C_{ro} (Wh K^{-1})	906	906	906	906
C_{ri} (Wh K^{-1})	16,866	16,866	16,866	16,866
R_{fo} (K W^{-1})	0.0003	0.0003	0.0003	0.0003
R_{fin} (K W^{-1})	0.0312	0.0312	0.0312	0.0312
R_{fi} (K W^{-1})	0.0095	0.0095	0.0095	0.0095
C_{fo} (Wh K^{-1})	839	839	839	839
C_{fi} (Wh K^{-1})	17,277	17,277	17,277	17,277
C_{air} (Wh K^{-1})	124	124	124	124
R_{pi} (K W^{-1})	0.0043	0.0043	0.0043	0.0043
C_p (Wh K^{-1})	11,774	11,774	11,774	11,774
f_w (-)	0.1542	0.1542	0.1542	0.1542
f_{wi} (-)	0.1107	0.1107	0.1107	0.1107
f_r (-)	0	0	0.1564	0.1564
f_{ri} (-)	0	0	0.1481	0.1481
f_f (-)	0.6717	0.6717	0	0
f_{fi} (-)	0.1481	0.1481	0	0
f_{ai} (-)	0.4	0.4	0.4	0.4
f_{pi} (-)	0.1564	0.1564	0.6717	0.6717

Table A8
Numerical values of the parameters for archetypes in class 1 (MFH in advanced refurbishment).

	Dwelling 1	Dwelling 2	Dwelling 3	Dwelling 4
Orientation	Ground floor (windows on perimeter walls facing north, south and west)	Ground floor (windows on perimeter walls facing north, south and east)	First floor (windows on perimeter walls facing north, south and west)	First floor (windows on perimeter walls facing north, south and east)
R_{winf} (K W^{-1})	0.0192	0.0192	0.0192	0.0192
R_{wo} (K W^{-1})	0.0013	0.0013	0.0013	0.0013
R_{win} (K W^{-1})	0.0686	0.0686	0.0686	0.0686
R_{wi} (K W^{-1})	0.0129	0.0129	0.0129	0.0129
C_{wo} (Wh K^{-1})	503	503	503	503
C_{wi} (Wh K^{-1})	8138	8138	8138	8138
R_{ro} (K W^{-1})	0.0008	0.0008	0.0008	0.0008
R_{rin} (K W^{-1})	0.0515	0.0515	0.0515	0.0515
R_{ri} (K W^{-1})	0.0068	0.0068	0.0068	0.0068
C_{ro} (Wh K^{-1})	958	958	958	958
C_{ri} (Wh K^{-1})	16,866	16,866	16,866	16,866
R_{fo} (K W^{-1})	0.0015	0.0015	0.0015	0.0015
R_{fin} (K W^{-1})	0.0546	0.0546	0.0546	0.0546
R_{fi} (K W^{-1})	0.0034	0.0034	0.0034	0.0034
C_{fo} (Wh K^{-1})	4361	4361	4361	4361
C_{fi} (Wh K^{-1})	4149	4149	4149	4149
C_{air} (Wh K^{-1})	124	124	124	124
R_{pi} (K W^{-1})	0.0043	0.0043	0.0185	0.0185
C_p (Wh K^{-1})	11,774	11,774	2741	2741
f_w (-)	0.1554	0.1554	0.1554	0.1554
f_{wi} (-)	0.1107	0.1107	0.147	0.147
f_r (-)	0	0	0.158	0.158
f_{ri} (-)	0	0	0.1967	0.1967
f_f (-)	0.6734	0.6734	0	0
f_{fi} (-)	0.1481	0.1481	0	0
f_{ai} (-)	0.4	0.4	0.4	0.4
f_{pi} (-)	0.158	0.158	0.6734	0.6734

Table A9
Numerical values of the parameters for archetypes in class 2 (MFH in existing state).

	Dwelling 1	Dwelling 2	Dwelling 3	Dwelling 4
Orientation	Ground floor (windows on perimeter walls facing north, south and west)	Ground floor (windows on perimeter walls facing north, south and east)	First floor (windows on perimeter walls facing north, south and west)	First floor (windows on perimeter walls facing north, south and east)
R_{winf} (K W^{-1})	0.0094	0.0094	0.0094	0.0094
R_{wo} (K W^{-1})	0.0014	0.0014	0.0014	0.0014
R_{win} (K W^{-1})	0.0184	0.0184	0.0184	0.0184
R_{wi} (K W^{-1})	0.0078	0.0078	0.0078	0.0078
C_{wo} (Wh K^{-1})	461	461	461	461
C_{wi} (Wh K^{-1})	2783	2783	2783	2783
R_{ro} (K W^{-1})	0.0006	0.0006	0.0006	0.0006
R_{rin} (K W^{-1})	0.0072	0.0072	0.0072	0.0072
R_{ri} (K W^{-1})	0.0054	0.0054	0.0054	0.0054
C_{ro} (Wh K^{-1})	1045	1045	1045	1045
C_{ri} (Wh K^{-1})	21,266	21,266	21,266	21,266
R_{fo} (K W^{-1})	0.0002	0.0002	0.0002	0.0002
R_{fin} (K W^{-1})	0.003	0.003	0.003	0.003
R_{fi} (K W^{-1})	0.0069	0.0069	0.0069	0.0069
C_{fo} (Wh K^{-1})	1016	1016	1016	1016
C_{fi} (Wh K^{-1})	18,615	18,615	18,615	18,615
C_{air} (Wh K^{-1})	156	156	156	156
R_{pi} (K W^{-1})	0.0035	0.0035	0.0035	0.0035
C_p (Wh K^{-1})	14435.56	14435.56	14435.56	14435.56
f_w (-)	0.1369	0.1369	0.1369	0.1369
f_{wi} (-)	0.0967	0.0967	0.0967	0.0967
f_r (-)	0	0	0.1678	0.1678
f_{ri} (-)	0	0	0.154	0.154

(*continued on next page*)

Table A9 (*continued*)

	Dwelling 1	Dwelling 2	Dwelling 3	Dwelling 4
f_f (-)	0.674	0.674	0	0
f_{fi} (-)	0.154	0.154	0	0
f_{ai} (-)	0.4	0.4	0.4	0.4
f_{pi} (-)	0.1678	0.1678	0.674	0.674

generalization of the results scaled to the entire Italian building stock.

The CFIs quantify the reserve of flexibility in terms of shiftable energy. They are calculated from the comparison between the flexible scenario and the baseline. The CFIs evaluated in terms of energy are the Cluster upward Shiftable Energy (CSE_{upward}) and the Cluster downward Shiftable Energy ($CSE_{downward}$). They quantify upward (i.e., increasing compared to the baseline) and downward (i.e., decreasing compared to the baseline) amount of shiftable energy due to the activation of flexibility in the cluster. CSE_{upward} and $CSE_{downward}$ are obtained according to Equations (8) and (9):

$$CSE_{upward} = \sum_{k}^{k_{tot}} \left[\dot{Q}_{FX}(k) - \dot{Q}_{BL}(k) \right] \Delta k \quad \text{if} \quad \dot{Q}_{FX}(k) \rangle \dot{Q}_{BL}(k) \tag{8}$$

$$CSE_{downward} = \sum_{k}^{k_{tot}} \left[\dot{Q}_{BL}(k) - \dot{Q}_{FX}(k) \right] \Delta k \quad \text{if} \quad \dot{Q}_{FX}(k) \langle \dot{Q}_{BL}(k) \tag{9}$$

SFIs are derived from CFIs by extending the quantification to the entire building stock. SFIs are evaluated both in terms of energy and power. In the first case, SFIs represent the average daily energy that can be moved (upwards or downwards) thanks to the activation of flexibility throughout the building stock. They are SSE_{upward} and $SSE_{downward}$, representing respectively the Stock upward Shiftable Energy and the Stock downward Shiftable Energy. SSE_{upward} and $SSE_{downward}$ are obtained by scaling the problem over the entire building stock according to Equations (10) and (11), where N_{cl} is the number of dwellings in the cluster, N_{st} is the number of dwellings in the entire building stock and d the number of days over which the CFIs are evaluated.

$$SSE_{upward} = \left(\frac{CSE_{upward}}{d} \right) \frac{N_{st}}{N_{cl}} \tag{10}$$

$$SSE_{downward} = \left(\frac{CSE_{downward}}{d} \right) \frac{N_{st}}{N_{cl}} \tag{11}$$

The SFIs in terms of power represent, on the other hand, the average and maximum power shiftable daily (upwards and downwards), obtained by the activation of flexibility in the entire building stock. These are the upward daily Average Stock Shiftable Power ($ASSP_{upward}$) and the downward daily Average Stock Shiftable Power ($ASSP_{downward}$), obtained dividing respectively Equations (10) and (11) by 24 h:

$$ASSP_{upward} = \left(\frac{SSE_{upward}}{24} \right) \tag{12}$$

$$ASSP_{downward} = \left(\frac{SSE_{downward}}{24} \right) \tag{13}$$

Finally, the daily Maximum Stock Shiftable Power ($MSSP_{upward}$) and the downward daily Maximum Stock Shiftable Power ($MSSP_{downward}$) belong also to the SFIs. They are calculated from the results of the clusters according to the Equations (14) and (15):

$$MSSP_{upward} = \max \left[\dot{Q}_{FX}(k) - \dot{Q}_{BL}(k) \right] \frac{N_{st}}{N_{cl}} \quad \text{if} \quad \dot{Q}_{FX}(k) \rangle \dot{Q}_{BL}(k) \tag{14}$$

$$MSSP_{downward} = \max \left[\dot{Q}_{BL}(k) - \dot{Q}_{FX}(k) \right] \frac{N_{st}}{N_{cl}} \quad \text{if} \quad \dot{Q}_{FX}(k) \langle \dot{Q}_{BL}(k) \tag{15}$$

3. Definition of scenarios for the italian residential building stock

This section describes the scenarios identified to represent the Italian building stock. Four scenarios are modelled: the first refers to the current composition of the Italian building stock (2020 scenario). Future scenarios are instead indicated with the names: 2030 scenario, 2040 scenario and 2050 scenario and respectively indicate the expected evolution of the Italian building stock in the decades 2020–2030, 2030–2040, and 2040–2050. The first subsection (3.1) describes the composition of the 2020 scenario, while the future scenarios are presented in subsection 3.2.

3.1. Definition of the current scenario

To obtain the current scenario, data from ISTAT (Italian National Statistical Institute) statistical surveys and from reports published by ENEA (Italian National Agency for new technologies, energy and sustainable economic development) were used and combined. Starting from the 15th ISTAT population and housing census [41], the number of residential buildings and dwellings divided by construction period and type of building is extrapolated (Table 1).

To obtain a limited number of archetypes that allow to represent the composition of the Italian building stock, some of the most representative cases have been identified. The construction periods modeled are before 1970 (class 1), from 1971 to 1990 (class 2), from 1991 to 2005 (class 3), from 2006 to 2015 (class 4) and from 2016 onwards (class 5). Instead, only two typologies of buildings have been modeled for each construction period: Single Family House (SFH), i.e., dwellings in single buildings, and Multi Family House (MFH), i.e., buildings with at least two dwellings. As the number of dwellings in each MFH is variable, the average number of dwellings per building for each construction period was evaluated. Moreover, since the 15th population census refers to surveys conducted in 2011, to obtain the number of the class 5, reference was made to [42], which shows statistical surveys on the number of buildings permits up to 2020. For the decade 2010–2020, ISTAT reports a total number of new residential buildings of 222′866, while total dwellings are 712′292, which correspond respectively to an average annual growth rate of 0.16% for buildings and 0.19% for dwellings. Table 2 summarizes the identified categories.

Considering the renovation rates reported in the Tabula project [43] and in the ENEA report [44], for each of the category identified in Table 2, three different states are defined: (i) existing state, (ii) usual refurbishment and (iii) advanced refurbishment. The difference between (ii) and (iii) lies in the level of thermal insulation and in the type of heating system. Only in advanced renovations HPs are envisaged. Furthermore, two types of emission system have been modeled in combination with the HPs: the first, with a lower thermal inertia, comparable to low temperature radiators, and the other with a higher thermal inertia, representative of underfloor heating. In this regard the following assumptions have been made:

- Dwellings of the construction period belonging to classes class 1, class 2 and class 3 with advanced renovation have the low thermal inertia emission system.
- Dwellings with HP of class 4 and class 5 have underfloor heating.

Table A10
Numerical values of the parameters for archetypes in class 2 (MFH in usual refurbishment).

	Dwelling 1	Dwelling 2	Dwelling 3	Dwelling 4
Orientation	Ground floor (windows on perimeter walls facing north, south and west)	Ground floor (windows on perimeter walls facing north, south and east)	First floor (windows on perimeter walls facing north, south and west)	First floor (windows on perimeter walls facing north, south and east)
R_{winf} (K W^{-1})	0.0133	0.0133	0.0133	0.0133
R_{wo} (K W^{-1})	0.0014	0.0014	0.0014	0.0014
R_{win} (K W^{-1})	0.0637	0.0637	0.0637	0.0637
R_{wi} (K W^{-1})	0.0078	0.0078	0.0078	0.0078
C_{wo} (Wh K^{-1})	481	481	481	481
C_{wi} (Wh K^{-1})	2783	2783	2783	2783
R_{ro} (K W^{-1})	0.0006	0.0006	0.0006	0.0006
R_{rin} (K W^{-1})	0.0322	0.0322	0.0322	0.0322
R_{ri} (K W^{-1})	0.0054	0.0054	0.0054	0.0054
C_{ro} (Wh K^{-1})	1166	1166	1166	1166
C_{ri} (Wh K^{-1})	21,266	21,266	21,266	21,266
R_{fo} (K W^{-1})	0.0002	0.0002	0.0002	0.0002
R_{fin} (K W^{-1})	0.0285	0.0285	0.0285	0.0285
R_{fi} (K W^{-1})	0.0069	0.0069	0.0069	0.0069
C_{fo} (Wh K^{-1})	1065	1065	1065	1065
C_{fi} (Wh K^{-1})	18,615	18,615	18,615	18,615
C_{air} (Wh K^{-1})	156	156	156	156
R_{pi} (K W^{-1})	0.0035	0.0035	0.0035	0.0035
C_p (Wh K^{-1})	14435.5556	14435.56	14435.5556	14435.56
f_w (-)	0.1369	0.1369	0.1369	0.1369
f_{wi} (-)	0.0967	0.0967	0.0967	0.0967
f_r (-)	0	0	0.1678	0.1678
f_{ri} (-)	0	0	0.154	0.154
f_f (-)	0.674	0.674	0	0
f_{fi} (-)	0.154	0.154	0	0
f_{ai} (-)	0.4	0.4	0.4	0.4
f_{pi} (-)	0.1678	0.1678	0.674	0.674

Table A11
Numerical values of the parameters for archetypes in class 2 (MFH in advanced refurbishment).

	Dwelling 1	Dwelling 2	Dwelling 3	Dwelling 4
Orientation	Ground floor (windows on perimeter walls facing north, south and west)	Ground floor (windows on perimeter walls facing north, south and east)	First floor (windows on perimeter walls facing north, south and west)	First floor (windows on perimeter walls facing north, south and east)
R_{winf} (K W^{-1})	0.0143	0.0143	0.0143	0.0143
R_{wo} (K W^{-1})	0.0014	0.0014	0.0014	0.0014
R_{win} (K W^{-1})	0.0809	0.0809	0.0809	0.0809
R_{wi} (K W^{-1})	0.0078	0.0078	0.0078	0.0078
C_{wo} (Wh K^{-1})	489	489	489	489
C_{wi} (Wh K^{-1})	2783	2783	2783	2783
R_{ro} (K W^{-1})	0.0006	0.0006	0.0006	0.0006
R_{rin} (K W^{-1})	0.0408	0.0408	0.0408	0.0408
R_{ri} (K W^{-1})	0.0054	0.0054	0.0054	0.0054
C_{ro} (Wh K^{-1})	1208	1208	1208	1208
C_{ri} (Wh K^{-1})	21,266	21,266	21,266	21,266
R_{fo} (K W^{-1})	0.0012	0.0012	0.0012	0.0012
R_{fin} (K W^{-1})	0.0421	0.0421	0.0421	0.0421
R_{fi} (K W^{-1})	0.0027	0.0027	0.0027	0.0027
C_{fo} (Wh K^{-1})	5499	5499	5499	5499
C_{fi} (Wh K^{-1})	5510	5510	5510	5510
C_{air} (Wh K^{-1})	156	156	156	156
R_{pi} (K W^{-1})	0.0035	0.0035	0.0167	0.0167
C_p (Wh K^{-1})	14435.5556	14435.5556	3045	3045
f_w (-)	0.1382	0.1382	0.1382	0.1382
f_{wi} (-)	0.0967	0.0967	0.1302	0.1302
f_r (-)	0	0	0.1699	0.1699

(*continued on next page*)

Table A11 (*continued*)

	Dwelling 1	Dwelling 2	Dwelling 3	Dwelling 4
f_{ri} (-)	0	0	0.2072	0.2072
f_f (-)	0.676	0.676	0	0
f_{fi} (-)	0.154	0.154	0	0
f_{ai} (-)	0.4	0.4	0.4	0.4
f_{pi} (-)	0.1699	0.1699	0.676	0.676

Table A12
Numerical values of the parameters for archetypes in class 3 (MFH in existing state).

	Dwelling 1	Dwelling 2	Dwelling 3	Dwelling 4	Dwelling 5
Orientation	Ground floor (windows on perimeter walls facing north, south and west)	First floor (windows on perimeter walls facing north, south and west)	First floor (windows on perimeter walls facing north, south and east)	Second floor (windows on perimeter walls facing north, south and west)	Second floor (windows on perimeter walls facing north, south and east)
R_{winf} (K W^{-1})	0.0087	0.0087	0.0087	0.0087	0.0087
R_{wo} (K W^{-1})	0.0047	0.0047	0.0047	0.0047	0.0047
R_{win} (K W^{-1})	0.0046	0.0046	0.0046	0.0046	0.0046
R_{wi} (K W^{-1})	0.0024	0.0024	0.0024	0.0024	0.0024
C_{wo} (Wh K^{-1})	11,597	11,597	11,597	11,597	11,597
C_{wi} (Wh K^{-1})	3440	3440	3440	3440	3440
R_{ro} (K W^{-1})	0.0003	0.0003	0.0003	0.0003	0.0003
R_{rin} (K W^{-1})	0.0051	0.0051	0.0051	0.0051	0.0051
R_{ri} (K W^{-1})	0.0024	0.0024	0.0024	0.0024	0.0024
C_{ro} (Wh K^{-1})	2366	2366	2366	2366	2366
C_{ri} (Wh K^{-1})	47,249	47,249	47,249	47,249	47,249
R_{fo} (K W^{-1})	0.0001	0.0001	0.0001	0.0001	0.0001
R_{fin} (K W^{-1})	0.0026	0.0026	0.0026	0.0026	0.0026
R_{fi} (K W^{-1})	0.0031	0.0031	0.0031	0.0031	0.0031
C_{fo} (Wh K^{-1})	2269	2269	2269	2269	2269
C_{fi} (Wh K^{-1})	41,358	41,358	41,358	41,358	41,358
C_{air} (Wh K^{-1})	347	347	347	347	347
R_{pi} (K W^{-1})	0.0018	0.001	0.001	0.0018	0.0018
C_p (Wh K^{-1})	27895.5833	53202.9167	53202.9167	27895.5833	27895.5833
f_w (-)	0.152	0.152	0.152	0.152	0.152
f_{wi} (-)	0.1096	0.0868	0.0868	0.1096	0.1096
f_r (-)	0	0	0	0.1775	0.1775
f_{ri} (-)	0	0	0	0.1581	0.1581
f_f (-)	0.6644	0	0	0	0
f_{fi} (-)	0.1581	0	0	0	0
f_{ai} (-)	0.4	0.4	0.4	0.4	0.4
f_{pi} (-)	0.1775	0.8419	0.8419	0.6644	0.6644

It is important to note that the two thermal emission systems make a significantly different contribution to the intrinsic thermal inertia of the building. In fact, by performing a response test on all archetypes, starting from an initial condition in which the heating system is switched off and the building is cold (i.e., all nodes are at the temperature of the external environment), an increase between 59 and 66 % of the time for achieving comfort (i.e., indoor air temperature of 21 °C) is observed in the highest inertia system compared with the lowest inertia system.

Finally, Fig. 2 shows the percentage composition of the Italian building stock in the scenario 2020 according to the identified categories. As can be seen, most of the dwellings belong to construction class 1 (53%) and class 2 (30%). Of these, only 41% have been renovated but not with advanced refurbishment. Considering the entire building stock, the percentage of houses with HPs in the 2020 scenario is very low, around 0.1%.

3.2. Definition of the future scenarios

To obtain future scenarios, the same annual growth rate of new constructions is assumed for the decade 2010–2020 (i.e., 0.19% annual average for dwellings as described in subsection 3.1). Furthermore, in line with the long-term renovation objectives of the building stock [34], an advanced renovation rate of 3% per year is assumed for the scenarios 2030 and 2040, while the value of 5% is selected for the 2050 scenario.

The following assumptions have been made to distribute new constructions and advanced refurbished dwellings in future scenarios:

- The new buildings have been attributed to the most recent class 5, with the characteristics of the building envelope of the class 5 (i.e., with advanced refurbishment and underfloor heating system).
- The percentage distribution between SFH and MFH in new buildings is assumed equal to that of the construction period class 5 for the 2020 scenario (i.e., 17 % SFH and 83 % MFH).
- The annual percentage of refurbishment is applied to each dwelling without HP (i.e., existing state and usual refurbishment), according to the cluster composition percentages identified in the 2020 scenario.
- The percentage of dwellings with a high inertia emission system has been assumed to increase in the various scenarios. It is assumed that in the 2030 scenario, 75% of refurbishment in the decade 2020–2030

Table A13
Numerical values of the parameters for archetypes in class 3 (MFH in usual refurbishment).

	Dwelling 1	Dwelling 2	Dwelling 3	Dwelling 4	Dwelling 5
Orientation	Ground floor (windows on perimeter walls facing north, south and west)	First floor (windows on perimeter walls facing north, south and west)	First floor (windows on perimeter walls facing north, south and east)	Second floor (windows on perimeter walls facing north, south and west)	Second floor (windows on perimeter walls facing north, south and east)
R_{winf} (K W^{-1})	0.0094	0.0094	0.0094	0.0094	0.0094
R_{wo} (K W^{-1})	0.0047	0.0047	0.0047	0.0047	0.0047
R_{win} (K W^{-1})	0.0153	0.0153	0.0153	0.0153	0.0153
R_{wi} (K W^{-1})	0.0024	0.0024	0.0024	0.0024	0.0024
C_{wo} (Wh K^{-1})	11,645	11,645	11,645	11,645	11,645
C_{wi} (Wh K^{-1})	3440	3440	3440	3440	3440
R_{ro} (K W^{-1})	0.0003	0.0003	0.0003	0.0003	0.0003
R_{rin} (K W^{-1})	0.0139	0.0139	0.0139	0.0139	0.0139
R_{ri} (K W^{-1})	0.0024	0.0024	0.0024	0.0024	0.0024
C_{ro} (Wh K^{-1})	2577	2577	2577	2577	2577
C_{ri} (Wh K^{-1})	47,249	47,249	47,249	47,249	47,249
R_{fo} (K W^{-1})	0.0001	0.0001	0.0001	0.0001	0.0001
R_{fin} (K W^{-1})	0.0117	0.0117	0.0117	0.0117	0.0117
R_{fi} (K W^{-1})	0.0031	0.0031	0.0031	0.0031	0.0031
C_{fo} (Wh K^{-1})	2356	2356	2356	2356	2356
C_{fi} (Wh K^{-1})	41,358	41,358	41,358	41,358	41,358
C_{air} (Wh K^{-1})	347	347	347	347	347
R_{pi} (K W^{-1})	0.0018	0.001	0.001	0.0018	0.0018
C_p (Wh K^{-1})	27895.5833	53202.9167	53202.9167	27895.5833	27895.5833
f_w (-)	0.152	0.152	0.152	0.152	0.152
f_{wi} (-)	0.1096	0.0868	0.0868	0.1096	0.1096
f_r (-)	0	0	0	0.1775	0.1775
f_{ri} (-)	0	0	0	0.1581	0.1581
f_f (-)	0.6644	0	0	0	0
f_{fi} (-)	0.1581	0	0	0	0
f_{ai} (-)	0.4	0.4	0.4	0.4	0.4
f_{pi} (-)	0.1775	0.8419	0.8419	0.6644	0.6644

envisages low inertia emission systems (i.e., similar to radiators), in the 2040 scenario 50% dwellings with underfloor heating system and 50% of dwellings with radiators have been assumed, and finally, in the 2050 scenario 100% of the dwellings renovated in the decade 2040–2050 are considered with underfloor heating system.

Fig. 3 shows the evolution of the composition of the building stock assessed for future scenarios. It is interesting to note that the total number of dwellings will increase by 12% compared to 2020. Furthermore, a significant decrease in dwellings that require advanced refurbishment can be observed. These are in fact 72% in 2030, 51% in 2040 and 29% in 2050. Fig. 4 instead shows the variation in terms of the number of dwellings with advanced refurbishment (i.e., with a HP). It can be highlighted how the total number of dwellings with heating systems based on HP is around 71 % of the total in the 2050 scenario, 49% in the 2040 scenario and 28% in the 2030 scenario. Moreover, moving from the decade 2020–2030 to the 2050 scenario, a progressive increase in the number of dwellings with a high thermal inertia emission system is observed. They are only 34% of dwellings with advanced refurbishment in the 2030 scenario while they become 46% and 65% respectively in the 2040 and 2050 scenarios.

4. Case study definition

The cluster modeled for each scenario is made up of 100 residential dwellings, considering both dwellings in SFH and MFH buildings. As anticipated, the construction characteristics of each archetype were obtained from the Tabula project [37]. All the thermal transmittances of the individual parts of the building envelope for the different construction classes considered respectively for SFH and MFH buildings are listed in Tables 3-6.

As anticipated, the numerical values of the parameters described in the model were obtained with a white box approach. In particular the procedure described in [45] has been applied on the basis of the constructive data of the selected archetypes. The numerical values of the parameters are given in the Appendix. With reference to Fig. 1, it is necessary to distinguish between the architecture of the RC-network used in the case of SFH and in the case of MFH:

- In the SFH building, all the building envelopes have been modeled as shown in Fig. 1 (i.e., introducing 2C and 3R for external perimeter walls, floor and roof).
- The thermal node (C_p, T_p) is instead used only for the MFH buildings. In fact, it contains building envelope surfaces that are not facing the external environment.
- For dwellings in MFH buildings, only the parts of the envelope facing outwards were modeled as 3R2C.

Concerning other important details, a climate file for the Italian city of Milan (45°27′40 N, 9°09′34 E) was used [46]. Furthermore, the energy price (c_e in Equation (5)) was assumed to be the price (PUN, Single National Price) of electricity sold in Italy in the year 2022 (Market of the day before) [47]. Finally, with regard to the limits imposed on the internal air temperature (Equations (3) and (6)), in the baseline scenario the temperature is kept close to the value of 21 °C. In the flexible scenario, however, the air temperature can be between 20 °C and 22 °C.

Table A14
Numerical values of the parameters for archetypes in class 3 (MFH in advanced refurbishment).

	Dwelling 1	Dwelling 2	Dwelling 3	Dwelling 4	Dwelling 5
Orientation	Ground floor (windows on perimeter walls facing north, south and west)	First floor (windows on perimeter walls facing north, south and west)	First floor (windows on perimeter walls facing north, south and east)	Second floor (windows on perimeter walls facing north, south and west)	Second floor (windows on perimeter walls facing north, south and east)
R_{winf} (K W^{-1})	0.0097	0.0097	0.0097	0.0097	0.0097
R_{wo} (K W^{-1})	0.0047	0.0047	0.0047	0.0047	0.0047
R_{win} (K W^{-1})	0.0214	0.0214	0.0214	0.0214	0.0214
R_{wi} (K W^{-1})	0.0024	0.0024	0.0024	0.0024	0.0024
C_{wo} (Wh K^{-1})	11,673	11,673	11,673	11,673	11,673
C_{wi} (Wh K^{-1})	3440	3440	3440	3440	3440
R_{ro} (K W^{-1})	0.0003	0.0003	0.0003	0.0003	0.0003
R_{rin} (K W^{-1})	0.0184	0.0184	0.0184	0.0184	0.0184
R_{ri} (K W^{-1})	0.0024	0.0024	0.0024	0.0024	0.0024
C_{ro} (Wh K^{-1})	2683	2683	2683	2683	2683
C_{ri} (Wh K^{-1})	47,249	47,249	47,249	47,249	47,249
R_{fo} (K W^{-1})	0.0005	0.0005	0.0005	0.0005	0.0005
R_{fin} (K W^{-1})	0.0189	0.0189	0.0189	0.0189	0.0189
R_{fi} (K W^{-1})	0.0012	0.0012	0.0012	0.0012	0.0012
C_{fo} (Wh K^{-1})	12,217	12,217	12,217	12,217	12,217
C_{fi} (Wh K^{-1})	12,243	12,243	12,243	12,243	12,243
C_{air} (Wh K^{-1})	347	347	347	347	347
R_{pi} (K W^{-1})	0.0018	0.0018	0.0018	0.0196	0.0196
C_p (Wh K^{-1})	27895.5833	27895.5833	27895.5833	2588.25	2588.25
f_w (-)	0.1524	0.1524	0.1524	0.1524	0.1524
f_{wi} (-)	0.1096	0.1096	0.1096	0.1488	0.1488
f_r (-)	0	0	0	0.1781	0.1781
f_{ri} (-)	0	0	0	0.2146	0.2146
f_f (-)	0.665	0	0	0	0
f_{fi} (-)	0.1581	0	0	0	0
f_{ai} (-)	0.4	0.4	0.4	0.4	0.4
f_{pi} (-)	0.1781	0.8431	0.8431	0.665	0.665

These values have been assumed in compliance with the conditions of hygrometric comfort expressed in [48]. The condition imposed was to not exceed the PPD (Predicted Percentage of Dissatisfied) of 10%. Finally, with regard to the modelling of the HP, as anticipated, performance was obtained from data declared by the manufacturer for a real air–water HP [40], while the size was chosen in relation to the design thermal load of the building. In particular, starting from the declared performance at certain operating points, the COP at all source temperatures was obtained by linear interpolation. Furthermore, it is important to highlight that, in order to maintain the linearity of the optimization problems, the load dependency of the COP was not modelled.

5. Results

In this section, the results of the flexibility characterization are presented. In this study the characterization of flexibility is applied only to the heating season and the results are evaluated over a reference winter period (i.e., the month of January) which has been shown to be sufficient to assess the differences between the different scenarios. For introductory purposes, the characterization of the flexibility of the clusters is preceded by a flexibility characterization that concerns individual buildings (subsection 5.1). In subsection 5.2 is presented the energy flexibility characterization of the scenarios for the clusters while in subsection 5.3 a generalization of the results to the entire building stock is proposed.

5.1. Evaluation of the energy flexibility of individual buildings with HPs

Before characterizing the impact of building stock refurbishment strategies on energy flexibility, it is useful to preliminarily evaluate how the two types of emission systems coupled to HPs (i.e., low and high thermal inertia) behave in terms of flexibility reserve. To do this, a single building (SFH) of class 3 with advanced refurbishment was considered. In one case, the building has the underfloor heating system (high thermal inertia of the emission system) and, in the other, the lowest thermal inertia system, which, as mentioned, represents low temperature radiators. Fig. 5 shows the characterization of flexibility according to the methodology introduced by [35].

Looking at the functional relationships between the energy price and the energy demand, a significantly different behavior in terms of flexibility for the two emission systems can be observed. In the building with higher thermal inertia emission system, the electricity demand seems to be able to adapt, with an almost linear trend, to price variations. On the other hand, in the building with lower thermal inertia emission system, a high price sensitivity is observed. In fact, for u greater than 0.4 (0.20 EUR kWh^{-1}) the energy demand tends to decrease by at least 50%.

The methodology of Junker et al [35] allows to evaluate the functional relationship with the state of charge. What emerged is a different tendency between the two buildings. The heating system with greater inertia tends to be more frequently in an average state of charge while the other one seems to prefer to be close to the upper boundary of the state of charge (almost 72 % of the charge). In general, a significant difference is also observed in terms of the share of flexible demand. This is equal to 50 % in the case of the building with the low inertia system, while it reaches 100 % for the building with the highest thermal inertia.

Table 7 shows the electricity consumption and bills for the two buildings analyzed. It can be noted that both buildings have a higher electricity consumption in the flexible scenario (1 % and 2 %

Table A15
Numerical values of the parameters for archetypes in class 4 (MFH in existing state).

	Dwelling 1	Dwelling 2	Dwelling 3	Dwelling 4	Dwelling 5
Orientation	Ground floor (windows on perimeter walls facing north, south and west)	First floor (windows on perimeter walls facing north, south and west)	First floor (windows on perimeter walls facing north, south and east)	Second floor (windows on perimeter walls facing north, south and west)	Second floor (windows on perimeter walls facing north, south and east)
R_{winf} (K W^{-1})	0.0236	0.0236	0.0236	0.0236	0.0236
R_{wo} (K W^{-1})	0.0141	0.0141	0.0141	0.0141	0.0141
R_{win} (K W^{-1})	0.0387	0.0387	0.0387	0.0387	0.0387
R_{wi} (K W^{-1})	0.0073	0.0073	0.0073	0.0073	0.0073
C_{wo} (Wh K^{-1})	3897	3897	3897	3897	3897
C_{wi} (Wh K^{-1})	1247	1247	1247	1247	1247
R_{ro} (K W^{-1})	0.001	0.001	0.001	0.001	0.001
R_{rin} (K W^{-1})	0.0469	0.0469	0.0469	0.0469	0.0469
R_{ri} (K W^{-1})	0.0072	0.0072	0.0072	0.0072	0.0072
C_{ro} (Wh K^{-1})	742	742	742	742	742
C_{ri} (Wh K^{-1})	8036	8036	8036	8036	8036
R_{fo} (K W^{-1})	0.0055	0.0055	0.0055	0.0055	0.0055
R_{fin} (K W^{-1})	0.0382	0.0382	0.0382	0.0382	0.0382
R_{fi} (K W^{-1})	0.0039	0.0039	0.0039	0.0039	0.0039
C_{fo} (Wh K^{-1})	7465	7465	7465	7465	7465
C_{fi} (Wh K^{-1})	2978	2978	2978	2978	2978
C_{air} (Wh K^{-1})	99	99	99	99	99
R_{pi} (K W^{-1})	0.0053	0.003	0.003	0.0053	0.0053
C_p (Wh K^{-1})	9653.7778	16871.5556	16871.5556	9653.7778	9653.7778
f_w (-)	0.1726	0.1726	0.1726	0.1726	0.1726
f_{wi} (-)	0.126	0.1019	0.1019	0.126	0.126
f_r (-)	0	0	0	0.1449	0.1449
f_{ri} (-)	0	0	0	0.142	0.142
f_f (-)	0.669	0	0	0	0
f_{fi} (-)	0.142	0	0	0	0
f_{ai} (-)	0.4	0.4	0.4	0.4	0.4
f_{pi} (-)	0.1449	0.8139	0.8139	0.669	0.669

respectively for lower and higher thermal inertia emission systems) while the cost drops in the flexible scenario by −1 % for the building with lower inertia emission system and −7 % for the building with higher inertia emission system. Furthermore, it is interesting to note that the building with underfloor heating has a much lower consumption than the one with the radiators, although the thermal and geometric characteristics of the building are the same. This obviously translates into a cheaper energy bill (Table 7).

5.2. Flexibility characterization of the representative clusters

As can be seen from the percentages in Fig. 2, the 2020 scenario does not envisage a percentage of dwellings with heat pumps higher than 0.5 %. For this reason, a negligible reserve of energy flexibility is assumed for the 2020 scenario. Fig. 6 shows the number of dwellings with HP for future scenarios, also highlighting the two types of emission systems (i.e., high and low thermal inertia). The number of dwellings with HPs gradually increases from the 2030 to the 2050 scenario. In fact, there are 26 dwelling with HP in the 2030 scenario (of which only 19 % with a high thermal inertia emission system), 47 in the 2040 scenario (of which the 45 % with a high thermal inertia emission system) and 72 in the 2050 scenario (of which 64 % with a high thermal inertia emission system).

The transition from one scenario to another has a significant impact on the quantification of the energy flexibility reserve. Fig. 7 shows the characterization of the energy flexibility of clusters in different future scenarios according to the methodology of [35]. The trend of the g(u) curve calculated for the different scenarios clearly shows the impact of the increase in the number of dwellings with HP and with high inertia heating system. Indeed, in accordance with Fig. 5, moving from the 2030 scenario to the 2050 scenario, the g(u) curve tends towards linearization. The differences appear less marked by observing the dependence of the cluster response on the general state of charge. In fact, all the cluster scenarios have shown a high yield to rather high charging states (i.e., about 71 %). Behavior more similar to that of the single building with low inertia emission system (subsection 5.1).

There were also significant differences in the share of flexible demand [35]. Passing from the 2030 scenario to the 2040 scenario and from the 2040 scenario to the 2050 scenario there is a progressive increase in the amount of energy that can be moved thanks to flexibility activation. In fact, the percentage of flexible demand is 61% in the 2030 scenario, 74% in the 2040 scenario and 80% in the 2050 scenario.

Table 8 shows the electricity consumption and bills for the future scenarios. It can be observed that the overall energy demand in the flexible scenario decreases with respect to the baseline. There is a reduction of −14% in the 2030 scenario, of −20% in the 2040 scenario and of −16% in the 2050 scenario. The electricity bill also undergoes important changes: −18%, –23% and −21% respectively for the 2030, 2040 and 2050 scenarios.

To evaluate the impact of activating energy flexibility, it is also important to assess if and how the peak in electricity demand changes. Looking at Fig. 8, only in the 2030 scenario there is a 2% increase in the peak of electricity demand in the flexible scenario compared to the baseline. This is obviously a rebound effect connected to a large flexibility activation. In the case of the cluster considered in 2030 scenario the peak difference is only 1 kW_e, however, it cannot be excluded that a large-scale activation of flexibility in a case like this can have not negligible consequences on the management of the grid.

Table A16
Numerical values of the parameters for archetypes in class 4 (MFH in usual refurbishment).

	Dwelling 1	Dwelling 2	Dwelling 3	Dwelling 4	Dwelling 5
Orientation	Ground floor (windows on perimeter walls facing north, south and west)	First floor (windows on perimeter walls facing north, south and west)	First floor (windows on perimeter walls facing north, south and east)	Second floor (windows on perimeter walls facing north, south and west)	Second floor (windows on perimeter walls facing north, south and east)
R_{winf} (K W^{-1})	0.0255	0.0255	0.0255	0.0255	0.0255
R_{wo} (K W^{-1})	0.0141	0.0141	0.0141	0.0141	0.0141
R_{win} (K W^{-1})	0.0546	0.0546	0.0546	0.0546	0.0546
R_{wi} (K W^{-1})	0.0073	0.0073	0.0073	0.0073	0.0073
C_{wo} (Wh K^{-1})	3905	3905	3905	3905	3905
C_{wi} (Wh K^{-1})	1247	1247	1247	1247	1247
R_{ro} (K W^{-1})	0.001	0.001	0.001	0.001	0.001
R_{rin} (K W^{-1})	0.0625	0.0625	0.0625	0.0625	0.0625
R_{ri} (K W^{-1})	0.0072	0.0072	0.0072	0.0072	0.0072
C_{ro} (Wh K^{-1})	777	777	777	777	777
C_{ri} (Wh K^{-1})	8036	8036	8036	8036	8036
R_{fo} (K W^{-1})	0.0055	0.0055	0.0055	0.0055	0.0055
R_{fin} (K W^{-1})	0.0434	0.0434	0.0434	0.0434	0.0434
R_{fi} (K W^{-1})	0.0039	0.0039	0.0039	0.0039	0.0039
C_{fo} (Wh K^{-1})	7469	7469	7469	7469	7469
C_{fi} (Wh K^{-1})	2978	2978	2978	2978	2978
C_{air} (Wh K^{-1})	99	99	99	99	99
R_{pi} (K W^{-1})	0.0053	0.003	0.003	0.0053	0.0053
C_p (Wh K^{-1})	9653.7778	16871.5556	16871.5556	9653.7778	9653.7778
f_w (-)	0.1726	0.1726	0.1726	0.1726	0.1726
f_{wi} (-)	0.126	0.1019	0.1019	0.126	0.126
f_r (-)	0	0	0	0.1449	0.1449
f_{ri} (-)	0	0	0	0.142	0.142
f_f (-)	0.669	0	0	0	0
f_{fi} (-)	0.142	0	0	0	0
f_{ai} (-)	0.4	0.4	0.4	0.4	0.4
f_{pi} (-)	0.1449	0.8139	0.8139	0.669	0.669

Finally, Fig. 9 shows the CFIs evaluated for the three future scenarios. These show the largest amount of energy that can be moved (both upwards and downwards) from the 2030 scenario to the 2050 scenario. The trend is also in line with the progressive increase in the penetration of HP among the scenarios (Fig. 6). Fig. 9 also shows how, with the same scenario, there is a greater amount of energy that can be moved down (CSE_{upward} is always less than $CSE_{downward}$). This is due to the fact that, since the optimization problem has the objective of minimizing the electric bill (Equation (5)), the lower bound for air temperature is always evaluated as more convenient (Equations (6) and (7)).

5.3. Flexibility characterization of the Italian building stock

In this section, a generalization of the results obtained for future scenarios to the entire Italian building stock is proposed. The objective is to assess how the long-term refurbishment strategies can have an impact on increasing the reserve of energy flexibility for the electricity grid. First, Fig. 10 shows the impact of the long-term refurbishment strategies on the reduction of overall thermal demand. This shows a quantification of the impact of such strategies on the reduction of energy demand for heating that, by 2050, reaches up to −38% in baseline scenario and −41 % in case of flexible scenario.

Fig. 11 reports the SFIs in terms of shiftable power calculated for the different scenarios of the Italian building stock. Fig. 11a shows the ASSP (Equation (12)) and the MSSP (Equation (14)) that can be shifted, increasing compared to the baseline, activating the flexibility of the entire building stock. On the other hand, Fig. 11b, represents the ASSP and MSSP calculated for decreasing power shifts compared to the baseline (respectively Equation (13) and Equation (15)). Considering the 2050 scenario, on average 4.7 GW_e can be moved downward and 1.9 GW_e upward, while a maximum shiftable power of at least 17.9 GW_e has been estimated both increasing and decreasing in comparison to the baseline. What is also interesting to observe by evaluating the evolution between the different future scenarios is the different growth rate of the ASSP and MSSP if the power shift takes place upwards or downwards. Indeed, the $ASSP_{upward}$ and $MSSP_{upward}$ increase by 19% and 44% from the 2030 scenario to 2040 and by 183% and 103% from the 2040 scenario to 2050. On the other hand, $ASSP_{downward}$ and $MSSP_{downward}$ increase by 142% and 119% from the 2030 scenario to 2040, whereas the corresponding increase is 77% and 50 % passing from the 2040 to the 2050 scenario. However, relating the average and maximum power shiftable to the Italian electricity demand in the year 2022 (minimum Italian electric power sold to the electricity market January 2022 about 190 GW [47]), these powers represent a percentage between −10% and + 9% in case of MSSP (-2%/+3% in 2030 scenario, −6%/+5% in 2040 scenario and −10%+9% in 2050 scenario) and between −2.5% and + 1% in case of ASSP (-0.8%/+0.3% in 2030 scenario, −1.7%/+0.4% in 2040 scenario and −2.5%+1% in 2050 scenario).

Fig. 12 instead reports the SFIs calculated in terms of shiftable energy (Equations (10) and (11)). The amount of daily energy that can be moved by activating the energy flexibility of the entire building stock goes from −34.4/+13.6 GWh_e in the 2030 scenario, to −75.4/+16.2 GWh_e in the 2040 scenario and up to −113.5/+45.8 GWh_e in the 2050 scenario. Considering the current Italian electricity demand, these numbers translate in terms of percentage referred to the minimum daily power demand [47] to percentage of shiftable energy of −0.6/+0.2 % in the 2030 scenario, of −1.3/+0.3 % in the 2040 scenario and up to −2/ +0.8 % in the 2050 scenario.

Table A17
Numerical values of the parameters for archetypes in class 4 (MFH in advanced refurbishment).

	Dwelling 1	Dwelling 2	Dwelling 3	Dwelling 4	Dwelling 5
Orientation	Ground floor (windows on perimeter walls facing north, south and west)	First floor (windows on perimeter walls facing north, south and west)	First floor (windows on perimeter walls facing north, south and east)	Second floor (windows on perimeter walls facing north, south and west)	Second floor (windows on perimeter walls facing north, south and east)
R_{winf} (K W^{-1})	0.0298	0.0298	0.0298	0.0298	0.0298
R_{wo} (K W^{-1})	0.0141	0.0141	0.0141	0.0141	0.0141
R_{win} (K W^{-1})	0.1366	0.1366	0.1366	0.1366	0.1366
R_{wi} (K W^{-1})	0.0073	0.0073	0.0073	0.0073	0.0073
C_{wo} (Wh K^{-1})	3946	3946	3946	3946	3946
C_{wi} (Wh K^{-1})	1247	1247	1247	1247	1247
R_{ro} (K W^{-1})	0.001	0.001	0.001	0.001	0.001
R_{rin} (K W^{-1})	0.1111	0.1111	0.1111	0.1111	0.1111
R_{ri} (K W^{-1})	0.0072	0.0072	0.0072	0.0072	0.0072
C_{ro} (Wh K^{-1})	883	883	883	883	883
C_{ri} (Wh K^{-1})	8036	8036	8036	8036	8036
R_{fo} (K W^{-1})	0.0019	0.0019	0.0019	0.0019	0.0019
R_{fin} (K W^{-1})	0.0938	0.0938	0.0938	0.0938	0.0938
R_{fi} (K W^{-1})	0.003	0.003	0.003	0.003	0.003
C_{fo} (Wh K^{-1})	3484	3484	3484	3484	3484
C_{fi} (Wh K^{-1})	4082	4082	4082	4082	4082
C_{air} (Wh K^{-1})	99	99	99	99	99
R_{pi} (K W^{-1})	0.0053	0.0053	0.0053	0.0208	0.0208
C_p (Wh K^{-1})	9653.7778	9653.7778	9653.7778	2436	2436
f_w (-)	0.1737	0.1737	0.1737	0.1737	0.1737
f_{wi} (-)	0.126	0.126	0.126	0.1651	0.1651
f_r (-)	0	0	0	0.1461	0.1461
f_{ri} (-)	0	0	0	0.186	0.186
f_f (-)	0.6702	0	0	0	0
f_{fi} (-)	0.142	0	0	0	0
f_{ai} (-)	0.4	0.4	0.4	0.4	0.4
f_{pi} (-)	0.1461	0.8163	0.8163	0.6702	0.6702

Although the flexibility characterization of the Italian building stock is very promising, some fundamental aspects should be highlighted. Firstly, as described, the results are obtained with reference to the actual Italian building stock. This can only make the results meaningful for the specific case study. However, as the assumed refurbishment rates are valid at EU level and the current composition of the Italian building stock can be compared to the actual average European building stock (according to Buildings Performance Institute Europe 97% of buildings in the EU need to be upgraded [36]), the results may also be significant for other EU countries. This is because the results can be representative of the potential flexibility reserve that can be achieved. This reserve can be scaled up and referred to other building stocks with current characteristics similar to the Italian case or considered as an upper limit for countries with a good number of flexible buildings at present.

Another aspect that needs to be emphasized concerns the limitations and assumptions made in the analysis. There are four main assumptions that can influence the results. These include: (i) The composition of the building stock in future scenarios; (ii) the focus only on the heating season; (iii) The participation rate of buildings in flexibility strategies; (iv) The electricity market characteristics.

The composition of the building stock in future scenarios (i), especially regarding the distribution of the type of emission system, may play a role in the quantification of flexibility indicators. However, the results clearly show greater responsiveness to flexibility strategies for buildings with higher thermal inertia emission system. This highlights the importance of providing sufficient levels of thermal inertia to decouple demand from generation in the renovation of heating systems in buildings. Although it is not easy to predict what will be the most common installation for emission systems in 2050, the assumptions regard the distribution of the emission systems foresees a spread of low temperature terminals in the future for highly refurbished buildings towards more efficient systems. As mentioned, the study deals only with the heating season (ii). The actual estimation of the potential flexibility reserve may vary during the cooling season due to the different penetrations of the electrically driven cooling systems and the types of emission systems used. Another assumption worth highlighting is the participation rate of buildings in the flexibility strategies (iii). This study assumes maximum involvement of all buildings equipped with HPs in flexibility strategies. This is obviously an ideal condition that can hardly be realized. However, it can represent the maximum reserve of flexibility obtainable from the building stock. Finally, as far as the electricity market is concerned (iv), the results refer to the current conditions of the Italian electricity market (both in terms of energy price and quantity of power/energy sold). However, in case of an important penetration of HPs in the domestic heating sector, these boundary conditions could undergo important variations. According to the results in the baselines for the clusters in future scenarios, Table 9 shows an estimate of the impact of the electricity demand of the HPs compared to the minimum electrical power sold in the current Italian electricity market [47]. It can be noted that, especially for the 2050 scenario, the share can reach 18% considering the maximum demand of HPs. This high penetration can therefore influence the dynamics of the electricity market. What is more, the buildings equipped with HP in this study are considered as price takers. In a scenario with a high penetration of HPs, buildings could also play a role as price makers. Such hypothetical changes in the electricity market can impact the absolute value of the results obtained. However, the overall findings of the analysis are not affected by this aspect.

The above critical discussion leads to the conclusion that the results

Table A18
Numerical values of the parameters for archetypes in class 5 (MFH in existing state).

	Dwelling 1	Dwelling 2	Dwelling 3	Dwelling 4	Dwelling 5
Orientation	Ground floor (windows on perimeter walls facing north, south and west)	First floor (windows on perimeter walls facing north, south and west)	First floor (windows on perimeter walls facing north, south and east)	Second floor (windows on perimeter walls facing north, south and west)	Second floor (windows on perimeter walls facing north, south and east)
R_{winf} (K W^{-1})	0.0255	0.0255	0.0255	0.0255	0.0255
R_{wo} (K W^{-1})	0.0141	0.0141	0.0141	0.0141	0.0141
R_{win} (K W^{-1})	0.0546	0.0546	0.0546	0.0546	0.0546
R_{wi} (K W^{-1})	0.0073	0.0073	0.0073	0.0073	0.0073
C_{wo} (Wh K^{-1})	3905	3905	3905	3905	3905
C_{wi} (Wh K^{-1})	1247	1247	1247	1247	1247
R_{ro} (K W^{-1})	0.001	0.001	0.001	0.001	0.001
R_{rin} (K W^{-1})	0.0625	0.0625	0.0625	0.0625	0.0625
R_{ri} (K W^{-1})	0.0072	0.0072	0.0072	0.0072	0.0072
C_{ro} (Wh K^{-1})	777	777	777	777	777
C_{ri} (Wh K^{-1})	8036	8036	8036	8036	8036
R_{fo} (K W^{-1})	0.0055	0.0055	0.0055	0.0055	0.0055
R_{fin} (K W^{-1})	0.0434	0.0434	0.0434	0.0434	0.0434
R_{fi} (K W^{-1})	0.0039	0.0039	0.0039	0.0039	0.0039
C_{fo} (Wh K^{-1})	7469	7469	7469	7469	7469
C_{fi} (Wh K^{-1})	2978	2978	2978	2978	2978
C_{air} (Wh K^{-1})	99	99	99	99	99
R_{pi} (K W^{-1})	0.0053	0.003	0.003	0.0053	0.0053
C_p (Wh K^{-1})	9653.7778	16871.5556	16871.5556	9653.7778	9653.7778
f_w (-)	0.1726	0.1726	0.1726	0.1726	0.1726
f_{wi} (-)	0.126	0.1019	0.1019	0.126	0.126
f_r (-)	0	0	0	0.1449	0.1449
f_{ri} (-)	0	0	0	0.142	0.142
f_f (-)	0.669	0	0	0	0
f_{fi} (-)	0.142	0	0	0	0
f_{ai} (-)	0.4	0.4	0.4	0.4	0.4
f_{pi} (-)	0.1449	0.8139	0.8139	0.669	0.669

presented in this work represent a potential estimation of future flexibility reserves considering the Italian scenario, but subject to the renovation policy at EU level, therefore the findings are relevant at European level. The results show that the planned strategies for the long-term energy upgrading of the building stock are extremely fruitful also from the point of view of energy flexibility.

6. Conclusions

In this work, a quantification of the potential flexibility reserve of reference residential building clusters is proposed. The objective is to assess the reserve of flexibility resulting from the entire building stock in the current scenario and in the future scenarios in which long-term refurbishment strategies have been applied.

Referring to the Italian case, clusters of 100 dwellings have been built considering the main archetypes representative of the most widespread residential dwellings in Italy. Four scenarios were modeled: the first related to the current scenario (scenario 2020), and the others related to the decades 2020–2030 (scenario 2030), 2030–2040 (scenario 2040) and finally the decade 2040–2050 (scenario 2050). The characterization of clusters in terms of energy flexibility has been conducted applying a methodology already available in literature and applied to individual buildings and through indicators of flexibility proposed by the authors. The quantification has been made both on the identified representative clusters and generalized to the entire building stock. The following points summarize the main considerations that emerged.

- The results have generally confirmed the improved capacity of high thermal inertia heating systems (e.g., underfloor heating systems) combined with heat pumps to activate energy flexibility (up to 100% of shiftable energy demand).
- The reference cluster representative of the current scenario has a negligible flexibility reserve.
- The reserve of energy flexibility increases significantly with the increase of renovated buildings. Indeed, the percentage of flexible demand become 61% in the 2030 scenario, 74% in the 2040 scenario and 80% in the 2050 scenario.
- The generalization of results to the entire Italian building stock has shown important reserves of flexibility that can be exploited by the management of demand for space heating. In terms of power, it has been obtained that by 2050 it is possible to have 17.9 GW_e (i.e., about 9% of the current Italian power base) of shiftable power (both increasing and decreasing). In terms of energy, the following daily average energies can be shifted if the flexibility reserve of the entire building stock is activated: $-34.4/+13.6$ GWh_e in the 2030 scenario (i.e., between -0.6% to 0.2% of the current Italian electricity demand), $-74.5/+16.2$ GWh_e in the 2040 scenario (i.e., between -1.3% to 0.3% of the current Italian electricity demand) and up to $-113.5/+45.8$ GWh_e in the 2050 scenario (i.e., between -2% to 0.8% of the current Italian electricity demand).

The results confirm the importance of the energy upgrading of the building stock also for the impact that it produces on the reserve of energy flexibility that is added to the entire energy system. It is important to underline that the results are strongly related to the current boundary conditions, especially as regards the electricity market. Therefore, they should be considered as a potential reserve estimate. However, they are relevant to be quantified in order to deepen the

Table A19
Numerical values of the parameters for archetypes in class 5 (MFH in advanced refurbishment).

	Dwelling 1	Dwelling 2	Dwelling 3	Dwelling 4	Dwelling 5
Orientation	Ground floor (windows on perimeter walls facing north, south and west)	First floor (windows on perimeter walls facing north, south and west)	First floor (windows on perimeter walls facing north, south and east)	Second floor (windows on perimeter walls facing north, south and west)	Second floor (windows on perimeter walls facing north, south and east)
R_{winf} (K W^{-1})	0.0298	0.0298	0.0298	0.0298	0.0298
R_{wo} (K W^{-1})	0.0141	0.0141	0.0141	0.0141	0.0141
R_{win} (K W^{-1})	0.1366	0.1366	0.1366	0.1366	0.1366
R_{wi} (K W^{-1})	0.0073	0.0073	0.0073	0.0073	0.0073
C_{wo} (Wh K^{-1})	3946	3946	3946	3946	3946
C_{wi} (Wh K^{-1})	1247	1247	1247	1247	1247
R_{ro} (K W^{-1})	0.001	0.001	0.001	0.001	0.001
R_{rin} (K W^{-1})	0.1111	0.1111	0.1111	0.1111	0.1111
R_{ri} (K W^{-1})	0.0072	0.0072	0.0072	0.0072	0.0072
C_{ro} (Wh K^{-1})	883	883	883	883	883
C_{ri} (Wh K^{-1})	8036	8036	8036	8036	8036
R_{fo} (K W^{-1})	0.0019	0.0019	0.0019	0.0019	0.0019
R_{fin} (K W^{-1})	0.0938	0.0938	0.0938	0.0938	0.0938
R_{fi} (K W^{-1})	0.003	0.003	0.003	0.003	0.003
C_{fo} (Wh K^{-1})	3484	3484	3484	3484	3484
C_{fi} (Wh K^{-1})	4082	4082	4082	4082	4082
C_{air} (Wh K^{-1})	99	99	99	99	99
R_{pi} (K W^{-1})	0.0053	0.0053	0.0053	0.0208	0.0208
C_p (Wh K^{-1})	9653.7778	9653.7778	9653.7778	2436	2436
f_w (-)	0.1737	0.1737	0.1737	0.1737	0.1737
f_{wi} (-)	0.126	0.126	0.126	0.1651	0.1651
f_r (-)	0	0	0	0.1461	0.1461
f_{ri} (-)	0	0	0	0.186	0.186
f_f (-)	0.6702	0	0	0	0
f_{fi} (-)	0.142	0	0	0	0
f_{ai} (-)	0.4	0.4	0.4	0.4	0.4
f_{pi} (-)	0.1461	0.8163	0.8163	0.6702	0.6702

knowledge on this resource and to strengthen the urgency towards important interventions in the residential building sector.

Declaration of Competing Interest

The authors declare that they have no known competing financial interests or personal relationships that could have appeared to influence the work reported in this paper.

Data availability

No data was used for the research described in the article.

Acknowledgement

This work is part of the research activities of the International Energy Agency Energy in Buildings and Communities Program Annex 82, Energy Flexible Buildings Towards Resilient Low Carbon Energy Systems.

The authors would like to thank Dr. Rune Grønborg Junker and the other authors of [35] *for the support in the application of their method for the energy flexibility characterization.*

APPENDIX

Numerical values of the RC-network parameters.

Table A1.
Table A2.
Table A3.
Table A4.
Table A5.
Table A6.
Table A7.
Table A8.
Table A9.
Table A10.
Table A11.
Table A12.
Table A13.
Table A14.
Table A15.
Table A16.
Table A17.
Table A18.
Table A19.

References

[1] IRENA (International Renewable Energy Agency). Energy Transition Holds Key to Tackle Global Energy and Climate Crisis. Available online (access verified June 28, 2023): https://www.irena.org/News/pressreleases/2022/Mar/Energy-Transition-Holds-Key-to-Tackle-Global-Energy-and-Climate-Crisis.
[2] European Commission. Energy and the Green Deal. Available online (access verified June 28, 2023): ec.europa.eu/info/strategy/priorities-2019-2024/european-green-deal/energy-and-green-deal_en.
[3] J. Blazquez, R. Fuentes-Bracamontes, C.A. Bollino, N. Nezamuddin, The renewable energy policy Paradox, Renewable and Sustainable Energy Reviews 82 (2018) 1–5.
[4] P. Neetzow, The effects of power system flexibility on the efficient transition to renewable generation, Applied Energy, Volume 283,116278, ISSN 0306–2619 (2021), https://doi.org/10.1016/j.apenergy.2020.116278.
[5] IRENA (2018), Power System Flexibility for the Energy Transition, Part 1: Overview for policy makers, International Renewable Energy Agency, Abu Dhabi.

Available online (access verified June 28, 2023): https://www.irena.org/publications/2018/Nov/Power-system-flexibility-for-the-energy-transition.
[6] European Commission. Energy efficiency in buildings. Available online (access verified June 28, 2023): https://ec.europa.eu/info/news/focus-energy-efficiency-buildings-2020-lut-17_en.
[7] H. Johra, P. Heiselberg, J.L. Dréau, Influence of envelope, structural thermal mass and indoor content on the building heating energy flexibility, Energy and Buildings 183 (2019) 325–339.
[8] G. Reynders, T. Nuytten, D. Saelens, Potential of structural thermal mass for demand-side management in dwellings, Building and Environment 64 (2013) 187–199.
[9] W. Li, L. Yang, Y. Ji, P. Xu, Estimating demand response potential under coupled thermal inertia of building and air-conditioning system, Energy and Buildings 182 (2019) 19–29.
[10] A. Mugnini, F. Polonara, A. Arteconi, Energy flexibility curves to characterize the residential space cooling sector: The role of cooling technology and emission system, Energy and Buildings, Volume 253, 111335, ISSN 0378–7788 (2021), https://doi.org/10.1016/j.enbuild.2021.111335.
[11] J. Niu, Z. Tian, Y. Lu, H. Zhao, Flexible dispatch of a building energy system using building thermal storage and battery energy storage, Applied Energy 243 (2019) 274–287.
[12] S. Stinner, K. Huchtemann, D. Müller, Quantifying the operational flexibility of building energy systems with thermal energy storages, Applied Energy 181 (2016) 140–154.
[13] Z. Luo, J. Peng, J. Cao, R. Yin, B. Zou, Y. Tan, J. Yan, Demand Flexibility of Residential Buildings: Definitions, Flexible Loads, and Quantification Methods, Engineering 16 (2022) 123–140.
[14] S.Ø. Jensen, A. Marszal-Pomianowska, R. Lollini, W. Pasut, A. Knotzer, P. Engelmann, A. Stafford, G. Reynders, IEA EBC Annex 67 Energy Flexible Buildings, Energy and Buildings 155 (2017) 25–34.
[15] A. Arteconi, A. Mugnini, F. Polonara, Energy flexible buildings: A methodology for rating the flexibility performance of buildings with electric heating and cooling systems, Applied Energy, Volume 251, 113387, ISSN 0306–2619 (2019), https://doi.org/10.1016/j.apenergy.2019.113387.
[16] J. Jasiūnas, P.D. Lund, J. Mikkola, Energy system resilience – A review, Renewable and Sustainable Energy Reviews, Volume 150, 111476, ISSN 1364–0321 (2021), https://doi.org/10.1016/j.rser.2021.111476.
[17] P.E. Roege, Z.A. Collier, J. Mancillas, J.A. McDonagh, I. Linkov, Metrics for energy resilience, Energy Policy 72 (2014) 249–256.
[18] R. Li, A.J. Satchwell, D. Finn, T.H. Christensen, M. Kummert, J. Le Dréau, R. A. Lopes, H. Madsen, J. Salom, G. Henze, K. Wittchen, Ten questions concerning energy flexibility in buildings, Building and Environment, Volume 223, 109461, ISSN 0360–1323 (2022), https://doi.org/10.1016/j.buildenv.2022.109461.
[19] S.H. Holmes, T. Phillips, A. Wilson, Overheating and passive habitability: indoor health and heat indices, Building Research & Information 44 (1) (2016) 1–19, https://doi.org/10.1080/09613218.2015.1033875.
[20] H. Tang, S. Wang, H. Li, F, lexibility categorization, sources, capabilities and technologies for energy-flexible and grid-responsive buildings: State-of-the-art and future perspective, Energy, Volume 219, 119598, ISSN 0360–5442 (2021), https://doi.org/10.1016/j.energy.2020.119598.
[21] S. Lo Piano, S.T. Smith, Energy demand and its temporal flexibility: Approaches, criticalities and ways forward, Renewable and Sustainable Energy Reviews, Volume 160, 112249, ISSN 1364–0321 (2022), https://doi.org/10.1016/j.rser.2022.112249.
[22] A. Kathirgamanathan, M. De, Rosa, E. Mangina, D.P. Finn, Data-driven predictive control for unlocking building energy flexibility: A review, Renewable and Sustainable Energy Reviews, Volume 135, 110120, ISSN 1364–0321 (2021), https://doi.org/10.1016/j.rser.2020.110120.
[23] I. Marotta, F. Guarino, M. Cellura, S. Longo, Investigation of design strategies and quantification of energy flexibility in buildings: A case-study in southern Italy, Journal of Building Engineering, Volume 41, 102392, ISSN 2352–7102 (2021), https://doi.org/10.1016/j.jobe.2021.102392.
[24] H. Li, Z. Wang, T. Hong, M.A. Piette, Energy flexibility of residential buildings: A systematic review of characterization and quantification methods and applications, Advances in Applied Energy, Volume 3, 100054, ISSN 2666–7924 (2021), https://doi.org/10.1016/j.adapen.2021.10005.
[25] G. Reynders, R. Amaral Lopes, A. Marszal-Pomianowska, D. Aelenei, J. Martins, D. Saelens, Energy flexible buildings: An evaluation of definitions and quantification methodologies applied to thermal storage, Energy and Buildings 166 (2018) 372–390.
[26] V.M. Nik, A. Moazami, Using collective intelligence to enhance demand flexibility and climate resilience in urban areas, Applied Energy, Volume 281, 116106, ISSN 0306–2619 (2021), https://doi.org/10.1016/j.apenergy.2020.116106.
[27] I. Vigna, R. Pernetti, W. Pasut, R. Lollini, New domain for promoting energy efficiency: Energy Flexible Building Cluster, Sustainable Cities and Society 38 (2018) 526–533.
[28] Ilaria Vigna, Roberto Lollini, Roberta Pernetti, Assessing the energy flexibility of building clusters under different forcing factors, Journal of Building Engineering, Volume 44, 2021, 102888, ISSN 2352-7102, https://doi.org/10.1016/j.jobe.2021.102888.
[29] K. Kaspar, M. Ouf, A. Ursula Eicker, critical review of control schemes for demand-side energy management of building clusters, Energy and Buildings, Volume 257, 111731, ISSN 0378–7788 (2022), https://doi.org/10.1016/j.enbuild.2021.111731.
[30] C. Papachristou, M.G.L.C. Pieter-Jan Hoes, T.A.J. van Loomans, J.L.M.H. Goch, Investigating the energy flexibility of Dutch office buildings on single building level and building cluster level, Journal of Building Engineering, Volume 40, 102687, ISSN 2352–7102 (2021), https://doi.org/10.1016/j.jobe.2021.102687.
[31] R. Tang, H. Li, S. Wang, A game theory-based decentralized control strategy for power demand management of building cluster using thermal mass and energy storage, Applied Energy 242 (2019) 809–820, https://doi.org/10.1016/j.apenergy.2019.03.152. ISSN 0306–2619,.
[32] A. Andrews, R.K. Jain, B. Energy, Efficiency: A clustering approach to embed demand flexibility into building energy benchmarking, Applied Energy, Volume 327, 119989, ISSN 0306–2619 (2022), https://doi.org/10.1016/j.apenergy.2022.119989.
[33] A. Amadeh, Z.E. Lee, K. Max Zhang, Building cluster demand flexibility: An innovative characterization framework and applications at the planning and operational levels, Energy Conversion and Management, Volume 283, 116884, ISSN 0196–8904 (2023), https://doi.org/10.1016/j.enconman.2023.116884.
[34] IEA (International Energy Agency). GlobalABC Roadmap for Buildings and Construction 2020-2050 Towards a zero-emission, efficient, and resilient buildings and construction sector. Available online (access verified June 28, 2023): https://www.iea.org/reports/globalabc-roadmap-for-buildings-and-construction-2020-2050.
[35] Rune Grønborg Junker, Carsten Skovmose Kallesøe, Jaume Palmer Real, Bianca Howard, Rui Amaral Lopes, Henrik Madsen, Stochastic nonlinear modelling and application of price-based energy flexibility, Applied Energy, Volume 275, 2020, 115096, ISSN 0306-2619, https://doi.org/10.1016/j.apenergy.2020.115096.
[36] Buildings Performance Institute Europe, 97% of buildings in the EU need to be upgraded. available online (access verified June 28, 2023): https://www.bpie.eu/wp-content/uploads/2017/12/State-of-the-building-stock-briefing_Dic6.pdf.
[37] V. Corrado, I. Ballarini, Stefano Paolo Corgnati, Building Typology Brochure-Italy, Fascicolo sulla Tipologia Edilizia Italiana, 2014 https://episcope.eu/fileadmin/tabula/public/docs/brochure/IT_TABULA_TypologyBrochure_POLITO.pdf.
[38] A. Boodi, K. Beddiar, Y. Amirat, M. Benbouzid, Simplified Building Thermal Model Development and Parameters Evaluation Using a Stochastic Approach, Energies 13 (11) (2020) 2899, https://doi.org/10.3390/en13112899.
[39] J. Neymark R. Judkoff M. Kummert R. Muehleisen A. Johannsen N. Kruis J. Glazer R. Henninger M. Witte E. Ono H. Yoshida Y. Jiang X. Zhou T. McDowell M. Hiller J. An D. Yan J. Allison P. Strachan Update of ASHRAE Standard 140 Section 5.2 and Related Sections (BESTEST Building Thermal Fabric Test Cases) 2020 N. p United States 10.2172/1643690 Web.
[40] Viessmann, VITOCAL 200-S, Commer. Cat. www.viessmann.it/it/riscaldamento-casa/pompe-di-calore/pompe-di-calore-aria-acqua-split/vitocal-200-s.html (access verified June 28, 2023).
[41] ISTAT (Italian national statistical institute). 15th Population and housing census. (2011). Available online (access verified June 28, 2023): https://www.istat.it/it/censimenti-permanenti/censimenti-precedenti/popolazione-e-abitazioni/popolazione-2011.
[42] ISTAT (Italian national statistical institute). Statistical survey of building permits. (2022). Available online (access verified June 28, 2023): https://www.istat.it/it/archivio/13020.
[43] Vincenzo Corrado, Ilaria Ballarini, Stefano Paolo Corgnati. D6.2 National scientific report on the TABULA activities in Italy (2012). ISBN: 978-88-8202-039-2. Available online (access verified June 28, 2023): https://episcope.eu/fileadmin/tabula/public/docs/scientific/IT_TABULA_ScientificReport_POLITO.pdf.
[44] Rossano Basili, Luca Colasuonno, Francesca Hugony, Francesca Pagliaro, Mauro Marani, Maurizio Matera, Fabio Zanghirella. Per CTI: Anna Martino, Giovanni Murano, Roberto Nidasio, Antonio Panvini. ENEA. Energy certification of buildings. Annual Report 2020. Available online (access verified June 28, 2023): https://www.efficienzaenergetica.enea.it/pubblicazioni/rapporto-annuale-sulla-certificazione-energetica-degli-edifici/rapporto-annuale-sulla-certificazione-energetica-degli-edifici-2020.html.
[45] A. Mugnini, G. Coccia, F. Polonara, A. Arteconi, Energy Flexibility as Additional Energy Source in Multi-Energy Systems with District Cooling, Energies. 14 (2) (2021) 519, https://doi.org/10.3390/en14020519.
[46] Climate.OneBuilding. Org, OneBuilding.Org. Repository of free climate data for building performance simulation. Available online (access verified June 28, 2023): https://climate.onebuilding.org/default.html.
[47] Manager of Italian electricity markets. Historical data available online (access verified June 28, 2023): https://www.mercatoelettrico.org/en/Statistiche/ME/DatiSintesi.aspx.
[48] O. Fanger Thermal Comfort 1970 Copenhagen.